Visual Neuroscience (2004), **21**, 567–586. Printed in the USA.
Copyright © 2004 Cambridge University Press 0952-5238/04 $16.00
DOI: 10.1017/S0952523804044074

The computational basis of an identified neuronal circuit for elementary motion detection in dipterous insects

CHARLES M. HIGGINS,[1,2] JOHN K. DOUGLASS,[1] AND NICHOLAS J. STRAUSFELD[1]

[1]Arizona Research Laboratories, Division of Neurobiology, University of Arizona, Tucson
[2]Department of Electrical and Computer Engineering, University of Arizona, Tucson

(RECEIVED September 15, 2003; ACCEPTED May 5, 2004)

Abstract

Based on comparative anatomical studies and electrophysiological experiments, we have identified a conserved subset of neurons in the lamina, medulla, and lobula of dipterous insects that are involved in retinotopic visual motion direction selectivity. Working from the photoreceptors inward, this neuronal subset includes lamina amacrine (α) cells, lamina monopolar (L2) cells, the basket T-cell (T1 or β), the transmedullary cell Tm1, and the T5 bushy T-cell. Two GABA-immunoreactive neurons, the transmedullary cell Tm9 and a local interneuron at the level of T5 dendrites, are also implicated in the motion computation. We suggest that these neurons comprise the small-field elementary motion detector circuits the outputs of which are integrated by wide-field lobula plate tangential cells. We show that a computational model based on the available data about these neurons is consistent with existing models of biological elementary motion detection, and present a comparable version of the Hassenstein-Reichardt (HR) correlation model. Further, by using the model to synthesize a generic tangential cell, we show that it can account for the responses of lobula plate tangential cells to a wide range of transient stimuli, including responses which cannot be predicted using the HR model. This computational model of elementary motion detection is the first which derives specifically from the functional organization of a subset of retinotopic neurons supplying the lobula plate. A key prediction of this model is that elementary motion detector circuits respond quite differently to small-field transient stimulation than do spatially integrated motion processing neurons as observed in the lobula plate. In addition, this model suggests that the retinotopic motion information provided to wide-field motion-sensitive cells in the lobula is derived from a less refined stage of processing than motion inputs to the lobula plate.

Keywords: Directional selectivity, Elementary motion detection, Lobula plate tangential cells, Visual motion, Insects

Introduction

A little more than 50 years ago, two researchers embarked upon a mathematical analysis of the behavior of the beetle *Chlorophanus*. They were investigating the optomotor response, a compensatory movement that many insects make in response to moving visual stimuli which serves to stabilize the visual environment. Among a small cadre of scientists using mathematical and physical interpretations of animal behaviors, they conducted experiments that allowed predictions about motor responses to a changing visual stimulus. A consequence of this work was the development of a simple mathematical model involving a correlation of signals from two neighboring visual sampling units (the set of photoreceptors that sample the same region of the visual field). This well-known set of experiments, carried out by Bernhard Hassenstein and Werner Reichardt (Hassenstein, 1950, 1951, 1958; Hassenstein & Reichardt, 1956), resulted in the mathematical model shown in Fig. 1. The Hassenstein-Reichardt (HR) correlation model, having been somewhat elaborated over the years (Van Santen & Sperling, 1985), continues to be used to explain optomotor reactions of insects (Reichardt et al., 1989; Pix et al., 2000).

Electrophysiological experimentation decades later (Dvorak et al., 1975; Hausen, 1982, 1984) led to the discovery of neurons in the lobula plate of flies which are sensitive to wide-field stimuli, direction-selective, and involved in optomotor control of the head and body. The motion responses of these cells, known as *tangential cells*, are also well predicted by the HR model (Egelhaaf et al., 1988). Because this response is synthesized from a relatively high-resolution retinal image, and because flies are clearly able to respond to small-field motion (Engelhaaf et al., 1993) it is natural to conclude that wide-field direction-selective cells integrate outputs from a large number of retinotopically organized small field direction-selective circuits, referred to in the literature as "elementary motion detectors" or EMDs (Franceschini et al., 1989; Egelhaaf et al., 1989; Krapp et al., 1998). Without the final time-

Address correspondence and reprint requests to: Charles M. Higgins, Electrical and Computer Engineering, University of Arizona, Tucson, AZ 85721, USA. E-mail: higgins@ece.arizona.edu.

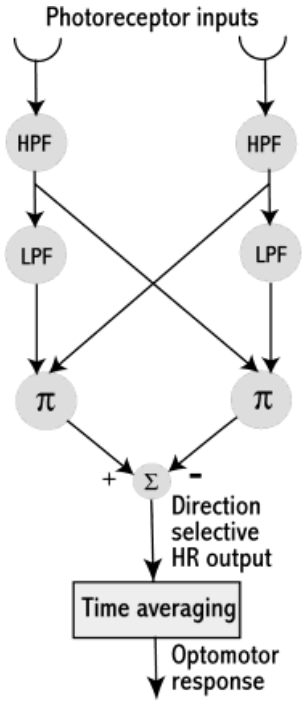

Fig. 1. Hassenstein-Reichardt (HR) model. Input from each visual sampling unit (filtered with a high-pass filter or HPF to remove the sustained illumination) is correlated (π indicates a multiplication) with a delayed (low-pass filter or LPF) version of the signal from a neighboring visual sampling unit. The difference (Σ indicates a summation) of left- and right-facing correlations results in a direction-selective output. The time-averaging step at the end is used when modeling optomotor responses or lobula plate tangential cells, but not elementary motion detection.

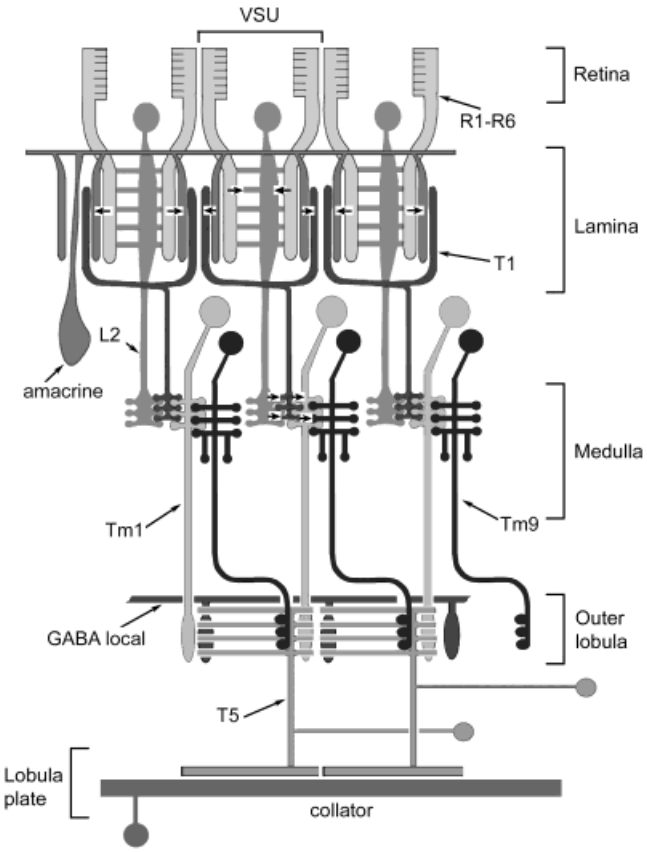

Fig. 2. Anatomical basis for proposed dipteran EMD circuit. Each visual sampling unit (VSU) is represented by a set of photoreceptors (R1-R6, here represented by a truncated pair) that synapse (arrows) onto amacrine cell processes and the dendrites of an L2 monopolar cell (L2). The basket-like arrangement of a T1 neuron is associated with set of receptor endings, and receives inputs from amacrine processes. The ending of the T1 neuron interposes between the terminal of L2 and the dendrites of two relay neurons, the transmedullary cell Tm1 and the GABA-immunoreactive neuron Tm9 (Sinakevitch & Strausfeld, 2004). These Tm cells end in a layer of the lobula complex where, in the presence of processes of a local GABA-immunoreactive neuron, they establish connections with dendrites of T5 neurons. T5 neurons show fully fledged responses to the orientation and direction of motion, and terminate on wide-field collator neurons in the lobula plate. T5 neurons occur as quartets and their endings segregate to four levels of the lobula plate, each encoding a different direction (Buchner & Buchner, 1984).

averaging step, the HR model can also be used to represent an EMD, and is widely used as a model of small-field outputs to wide-field direction-selective cells in insects (Harris et al., 1999).

Despite the fifty-odd years since the formulation of the HR model, and many highly successful mathematical refinements of the model, the *neuronal basis* for elementary motion detection in insects is still an open question even though the retinotopic nature of inputs onto wide-field tangentials in the lobula plate has been verified anatomically (Strausfeld & Lee, 1991) and electrophysiologically (Douglass & Strausfeld, 1995). The computation that is being performed is well represented as a whole by the HR model, but the neuronal structure that connects photoreceptors to lobula plate tangential cells does not obviously equate to the HR model. Direct electrophysiological exploration of this question is hampered by the extremely small size of the axons which must be penetrated to obtain recordings, and by the daunting complexity of the neuropils in which they are located. For this reason, rather few recordings exist from insect neurons that might be candidate elementary motion detectors (Douglass & Strausfeld, 1995, 1996; James & Osorio, 1996).

In the fly optic lobes, there are more than 40 unique anatomically identifiable types of retinotopic neurons (Strausfeld, 1976), each type probably present in each structural unit—an optic cartridge or column—representing a visual sampling unit of the retina. Comparative studies among many species of flies, and between honey bees and sphingid hawkmoths, have determined that a subset of these neurons (Fig. 2) is ubiquitously conserved across evolutionarily divergent neopteran insect groups (Strausfeld, 1976; Buschbeck & Strausfeld, 1996; Wicklein & Strausfeld, 2000). Starting at the periphery, this neuronal subset includes lamina amacrine (α) cells, lamina monopolar (L2) cells, an efferent neuron with basket-like dendrites called the T-cell (T1 or β), a neuron that relays information through the second synaptic neuropil of the medulla—the transmedullary cell Tm1, and the T5 bushy T-cell the dendrites of which are disposed in a superficial layer of the third synaptic neuropil, the lobula, and whose axons terminate in the tectum-like neuropil of the lobula plate.

Measurements across different taxa showing consistent depth relationships among homologues of these neurons imply likely connections among them at their second and third synaptic levels (Buschbeck & Strausfeld, 1996). Intracellular recordings and dye fills obtained from the fly optic lobes have identified many of these

cells' stimulus preferences and response characteristics (Douglass & Strausfeld, 1995, 1996). Histological studies have also identified some putative neurotransmitters, their precursors, or possible receptors employed at various levels (Sinakevitch & Strausfeld, 2004).

Electron-microscopical observations at the level at which photoreceptor neurons terminate have revealed connections among photoreceptor terminals, local amacrine cells, and three types of lamina monopolar neurons, including the L2 cells (Strausfeld & Campos-Ortega, 1977), which like the type 1 amacrine cells are directly postsynaptic to achromatic photoreceptors that end at each optic cartridge (Boschek, 1971; Campos-Ortega & Strausfeld, 1973; Strausfeld & Campos-Ortega, 1977).

Amacrine cells are prominent elements of the lamina, supplying processes across the whole neuropil and around each columnar group of receptor endings denoting each optic cartridge. It is conceivable that amacrine cells form an isomorphic network of functionally connected elements (see Discussion) supporting input from photoreceptor terminals at many optic cartridges. One definitive recording has been obtained from an amacrine cell of the green bottle fly *Phaenicia sericata*, identified as such by dye injection (Douglass & Strausfeld, 2004). The cell showed a steady depolarizing response to both transient and sustained illumination over stimulation periods as long as 500 ms, and a noninverting response to light intensity. Amacrine cells project to surrounding optic cartridges, where they have been shown to synapse onto the basket-like dendrites of T1 cells. In the medulla, the terminals of T1 cells are contacted by the endings of the L2 monopolar cells from the same optic cartridge (Campos-Ortega & Strausfeld, 1973), both terminals being embraced by the dendrites of Tm1 cells. This organization is repeated across the whole lamina and medulla.

L2 cells respond to an increase in illumination by hyperpolarizing and have no significant response to sustained illumination (Coombe et al., 1989). Significant electrophysiological data, including details of frequency response (Laughlin, 1984; Coombe et al., 1989), are available for this cell, revealing a roughly bandpass temporal-frequency characteristic.

Neuroanatomical studies identify two types of transmedullary cells the dendrites of which reside at the level of T1 and L2 endings. These are the aforementioned type 1 transmedullary cell Tm1, and the type 9 transmedullary cell Tm9 (Fischbach & Dittrich, 1989; Douglass & Strausfeld, 1998). Their axons extend the series of relays from receptor terminals to T5 cells. Limited electrophysiological data on Tm1 is available (Figs. 6 and 7, middle traces). In response to a flicker stimulus, Tm1 shows a strong response to transient stimulation with a small response to sustained illumination. When presented with moving gratings, Tm1 did not show a directionally dependent increase or decrease in mean membrane potential. However, it did appear to show a weak frequency doubling, analyzed in Douglass and Strausfeld (1995). The peripheral dendrites of the Tm9 neuron, which is GABA immunoreactive (Sinakevitch & Strausfeld, 2004), are disposed to receive inputs from Tm1. Tm9 terminates in the lobula at the layer of T5 cell dendrites, *via* a displacement of its axon by a single retinotopic column interval.

T5 cells are unusual in that they are arranged as quartets, with four T5 cells for each visual sampling unit. Their dendrites also overlap in the lobula and each quartet sends out four axons that terminate at four levels in the lobula plate. T5 endings are almost certainly presynaptic to lobula plate tangentials (Strausfeld & Lee, 1991). The tendency of T5 cell terminals to segregate into four layers corresponds to each layer's directional selectivity to moving gratings, as shown by activity staining with ^{3}H-deoxyglucose (Buchner et al., 1979; Bausenwein & Fischbach, 1992). Electrophysiological recordings (Douglass & Strausfeld, 1995) show that the T5 cell represents directional motion in its mean response (Fig. 10, bottom trace). Anatomical details (N. J. Strausfeld, unpublished observations, 2002) suggest that transmedullary (Tm) inputs from a number of neighboring optic cartridges on either side of each T5 are integrated to produce a motion output. Also shown in Fig. 2 is a GABA-immunoreactive local interneuron identified in a recent histological study as restricted to the T5 dendritic layer (Sinakevitch & Strausfeld, 2004). This neuron receives inputs at the same level as T5 cells and is assumed to provide inhibition at the T5 level (see Methods).

Most of the current predictions of the properties of EMDs (Franceschini et al., 1989; Coombe et al., 1989; Egelhaaf & Borst, 1989; Borst, 2001; Borst & Haag, 2002) have been inferred indirectly from responses of lobula plate tangential cells, which are relatively large and easier to record from. Franceschini et al. (1989) conducted an experiment aimed specifically at determination of the nature of elementary motion detection. While the activity of a tangential cell reflects the sum of multiple EMD outputs, if it were possible to stimulate only a single EMD, the recording from a tangential cell would reveal the physiology of the EMD circuit. This was accomplished by the use of a complex microscope-telescope stimulator, exploiting the sophisticated neural superposition eye of the fly (Nilsson, 1989). Franceschini et al. were able to record from an H1 tangential cell while optically stimulating two adjacent but optically divergent photoreceptors in a controlled sequence, thereby activating two neighboring optic cartridges. Egelhaaf and Borst (1989) studied the intracellular responses of horizontal system (HS) tangential cells to sinusoidal grating stimuli which were initially stationary and then began moving suddenly in the null direction. The (nonspiking) membrane potential responses observed include a transient "ringing" oscillation at the pattern temporal frequency. These transient oscillations (but not several other features of the HS cell response, including a transient depolarization and an adaptation to sustained motion) were well predicted by the HR model. Coombe et al. published a study in 1989 considering whether large monopolar cells (LMCs) could be part of the optomotor pathway (and thus part of the EMD). A number of results from these studies are germane to the present work.

With the goal of advancing testable hypotheses to guide further biological experimentation, this volume of anatomical and physiological data is used here to show that a computational model of insect retinotopic neurons, synthesizing the available data regarding response properties and assumed synaptic relationships, results in a response to moving visual stimuli with properties comparable to the HR model, and consistent with previous predictions of the properties of EMDs. We propose that small-field visual motion is computed in two distinct stages. Computed first in the visual processing chain is a representation of *nondirectional motion* as suggested by the responses of Tm1 cells. Nondirectional motion units respond to moving stimuli in a particular band of spatial and temporal frequency, but without regard to direction. The second stage of motion detection is the computation of *directional motion*, identified with T5 cells, through the integration of the responses of a spatial pattern of nondirectional motion units. Directional motion units are responsive to moving stimuli within a range of spatial and temporal frequency, and are selective for motion along a particular preferred direction.

Materials and methods

Simulations of the computational models were carried out using the *Matlab* package (The Mathworks, Natick, MA). All of the simulations incorporated two spatial dimensions; that is, the simulated visual input to the motion detector array could be expressed as a two-dimensional image that changes over time.

Unless otherwise specified, the following parameters were used for each simulation. Each simulation incorporated a 40 × 40 pixel image viewed by a 20 × 20 hexagonal array of photoreceptors, incorporating a similar number of EMD models, of which several rows and columns at the periphery on each side were not completely functional due to missing photoreceptor inputs. Simulation experiments were performed with a fixed timestep of 10 ms, which we observed to be small enough relative to all filter time constants that the simulation was numerically stable. Since the model is entirely feedforward, there is no possibility of inherent instability in the simulations. Experiments ran for simulated times up to 10 s.

Details of our implementation of EMD models and a generic tangential cell and descriptions of the stimuli for each experiment are given below.

Neuronally based EMD model details

Refer to Fig. 3a for a block diagram of the one-dimensional neuronally based EMD model; the two-dimensional version of the model was used for all simulations (see Results). Justification for the model is given in Results.

Model photoreceptors are optically arranged in a hexagonal array and report the luminance averaged over small nonoverlapping spatial patches (2 × 2 image pixels for the standard simulation size) of the input image centered at their spatial position.

The L2 cell is modeled as a *negative* first-order high-pass filter (HPF) with a time constant of 50 ms.

Amacrine cells in the model receive input from the local photoreceptor only and respond identically to the photoreceptor. The model amacrine-T1 synapse, however, includes a "relaxed" high-pass filter (specifics below) and a sign inversion.

The synapse of L2 onto the T1 axon close to the Tm1 synapse is modeled as a direct synapse from L2 to Tm1. A first-order low-pass filter (LPF) with a time constant of 50 ms is included in the path from the amacrine cell to T1, with T1 being modeled as a summation.

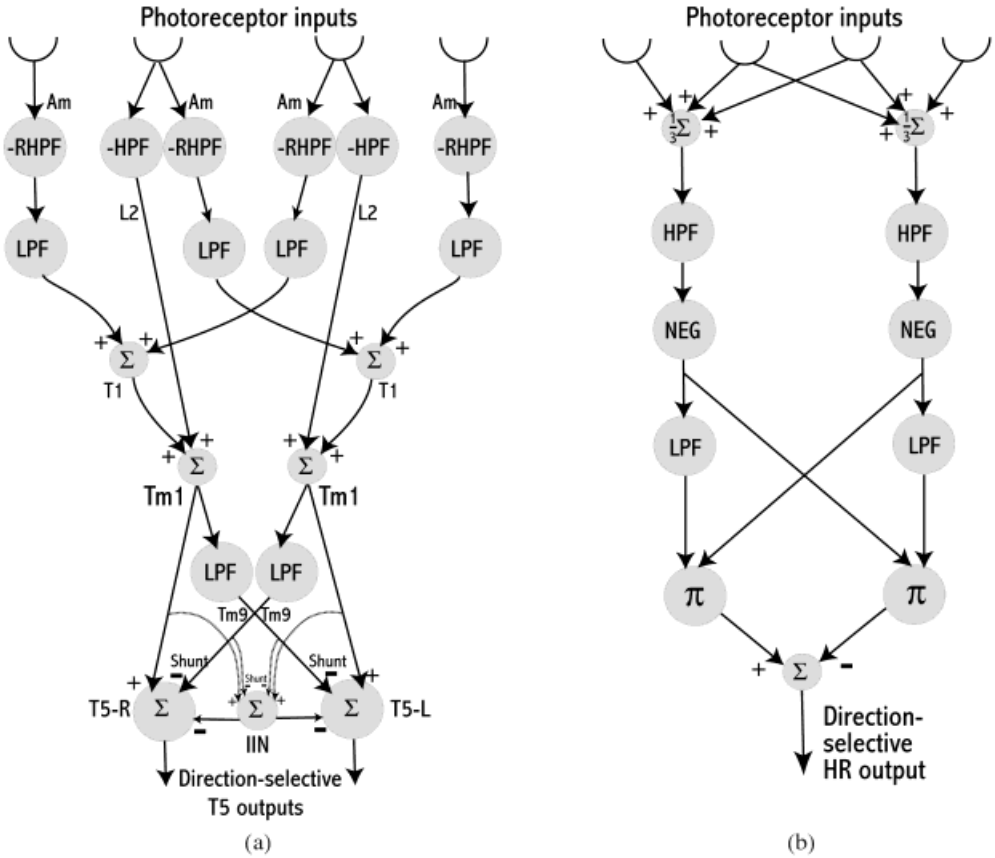

Fig. 3. Computational models of directional motion units. (a) Neuronally based one-dimensional computational EMD model ending with direction-selective T5 units. HPF indicates high-pass filtering; RHPF indicates "relaxed" high-pass filtering allowing a small sustained response (see Methods). LPF indicates low-pass filtering. Σ indicates a sum. The rectification inherent in the shunting inhibition expression makes the T5 units sensitive to transiently decreasing intensity levels only. In the two-dimensional version of the model, each T1 unit takes low-pass filtered inputs from all six surrounding optic cartridges, rather than just the left and right neighbors as shown above. IIN indicates the inhibitory interneuron at the T5 level. (b) Comparable HR model incorporating a rectification step. The NEG operator is rectifying, passing only the negative part of the signal. π indicates a product. In order to match the spatial-frequency response of the neuronally based EMD model, it is necessary to average neighboring photoreceptor inputs in the HR model as shown.

Tm1 is modeled as simply summing L2 and T1 inputs. Tm9 receives the same inputs as Tm1, but is additionally delayed with respect to Tm1 by a first-order low-pass filter with a time constant of 100 ms.

T5 is believed to integrate Tm inputs from a number of neighboring optic cartridges on either side to produce a motion output. The simulated version of the model combines local Tm cells with those from a neighboring optic cartridge. The relative orientation of these two optic cartridges determines the preferred-null axis of the resulting T5 cells. Model Tm1 and Tm9 cells converge onto a T5 cell, with Tm9 crossing to a neighboring optic cartridge. Tm1 excites T5 cells, whereas Tm9 synapses onto T5 with a shunting inhibitory connection (specifics below). An inhibitory interneuron receives the same inputs as both T5 cells combined (including excitatory Tm1 and shunting inhibitory Tm9 inputs) and inhibits both T5 cells; thus its activation is subtracted from both T5 cells (specifics below).

Relaxed high-pass filtering

It is necessary for the high-pass filter at the amacrine-T1 synapse to allow a small sustained response component. In the Laplace transform domain, the transfer function of a first-order high-pass filter may be expressed as

$$H_{HPF}(s) = \frac{s\tau}{1 + s\tau}, \tag{1}$$

which has no response to sustained signals. To allow a small component of sustained signal to pass, we add a weighted low-pass filter function as shown below.

$$H_{RHPF}(s) = \frac{s\tau}{1 + s\tau} + k \cdot \frac{1}{1 + s\tau} = k \cdot \frac{1 + s\tau_2}{1 + s\tau}, \tag{2}$$

where $\tau_2 = \tau/k$. This function still has the general characteristics of a high-pass filter, but additionally has a small response of magnitude k to sustained inputs. For our experiments, τ was 50 ms and k was set to 0.1.

Shunting inhibition

A mathematical expression for shunting (silent) inhibition in the presence of a single excitatory input is required to compute the effects of the model Tm cells on the model T5. A shunting inhibitory input can reduce the effects of an excitatory input, but not hyperpolarize the cell.

A simple model of shunting inhibition can be obtained by considering it as a "dirty multiplication" (Torre & Poggio, 1978; Koch, 1999), in which the effect on an excitatory input I_e is expressed as a multiplication by a number which reaches zero when the shunting inhibitory input I_s is at its positive maximum, and is unity for no shunting input:

$$S(I_e, I_s) = \mathrm{pos}(I_e) \cdot \left(1 - \frac{\mathrm{pos}(I_s)}{I_{smax}}\right), \tag{3}$$

where S, I_e, and I_s, respectively, represent the cellular membrane potential, an excitatory input, and a shunting input. I_{smax} represents the maximum positive value reached by I_s, and thus $\mathrm{pos}(I_s)/I_{smax}$ represents the normalized ion channel conductance of the shunting inhibitory input. The "*pos*" operator indicates a rectification (the positive part only is taken), required because ion channel conductance cannot be negative.

The inhibitory interneuron

The inhibitory interneuron used in the neuronally based EMD model receives the same inputs as the two T5 cells combined and returns a weighted inhibition to both. Mathematically, this is expressed as

$$T5'_L = T5_L - a \cdot (T5_L + T5_R),$$

$$T5'_R = T5_R - a \cdot (T5_L + T5_R), \tag{4}$$

where a is a constant, $T5_L$ and $T5_R$ represent the inputs to the two T5 cells (including the effects of both the excitatory Tm1 and shunting inhibitory Tm9 cells), and $T5'_L$ and $T5'_R$ represent their activities with inhibition. For the special case $a = 0.5$ (used in all simulations shown), the T5 outputs represent a "balanced" difference of the two T5 cell inputs:

$$T5'_L = 0.5 \cdot (T5_L - T5_R),$$

$$T5'_R = 0.5 \cdot (T5_R - T5_L). \tag{5}$$

HR model details

Refer to Fig. 3b for a block diagram of the one-dimensional HR model. Justification for the model is given in Results.

High-pass filters used in the model were, as in the neuronally based EMD model, first order with a time constant of 50 ms. The low-pass filter used was second order (see Results), constructed as the convolution of the two low-pass filters used in the neuronally based EMD model, with time constants of 50 ms and 100 ms.

Generic tangential cell model

To test the neuronally based EMD model against predictions from tangential cells, we use EMDs to synthesize a rudimentary spiking tangential cell, diagrammed in Fig. 4. We first spatially sum the outputs of EMD models from all optic cartridges in our simulation. This quantity might represent the subthreshold membrane potential, without action potentials. To this quantity is added a constant to represent the spontaneous firing rate of the cell. Finally, this value is rectified (negative quantities become zero) to represent the firing rate of the simulated tangential cell. For maximum generality, the T1 units used in this model are not orientation selective (that is, T1 sums the entire hexagonal surround) although the T5 units are by necessity orientation and direction selective.

Visual stimuli

Visual stimuli were chosen to facilitate comparisons of the responses of the present model to those of the HR model, and to previously published electrophysiological recordings that have been used to predict properties of the fly's EMDs (see Results).

Drifting sinusoidal gratings

Drifting sinusoidal gratings were used to characterize the spatiotemporal frequency response of EMD models. Sinusoidal visual stimuli were computed as

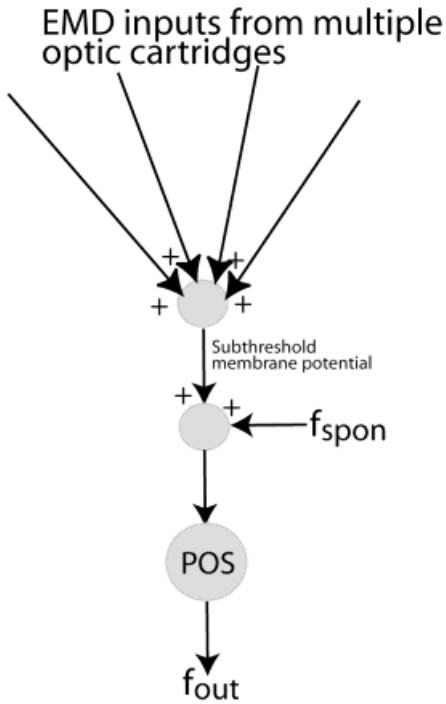

Fig. 4. Integration of neuronally based EMD model outputs into a generic tangential cell by spatial summation, addition of a constant (f_{spon}, the spontaneous firing rate), and finally half-wave rectification (POS). The final output f_{out} represents the *firing rate* of the tangential cell.

$$I(x, y, t) = \frac{1}{2} \cdot (1 + C \cdot \sin(\omega_t \cdot t + \omega_x \cdot x + \omega_y \cdot y + \phi)), \qquad (6)$$

where t indicates time, C is the contrast, ω_t is the temporal frequency, ω_x, ω_y are the spatial frequencies, and ϕ is the initial phase. The direction of the stimulus is indicated by the sign of the temporal frequency. The two-dimensional orientation is implicitly expressed in the spatial frequencies. The stimulus velocity is implicit in the ratio of temporal to spatial frequencies.

Impulses and steps

Flashing stimuli comparable to those used in Franceschini et al. (1989) were used to evaluate EMD model properties. Both step and impulse stimuli were one image pixel square (i.e. spatially as small as possible). Since the HR and neuronally based EMD models as developed in the text respond only to transiently decreasing intensity levels, impulse stimuli were normally unity (on a background of unity intensity) and changed to a value of zero for a single timestep. Step stimuli went from unity to zero between one timestep and the next.

Transiently moving sinusoidal gratings

Initially static sinusoidal gratings which abruptly began moving and later stopped were used to compare model responses to data from Egelhaaf and Borst (1989). The results of this experiment exhibited a strong dependence on the initial phase of the sinusoid grating, and so it was necessary to vary the initial phase randomly, and average both over multiple experiments and over a number of simulated EMDs. Because the stimulus moved in the horizontal direction only, model cells vertically placed with respect to one another responded identically. For this reason, these simulations were performed using 100×10 images, and a 50×5 hexagonal array of photoreceptors, all of the functional units of which were integrated into a generic tangential cell. To further remove the effects of the initial phase of the grating stimulus, the phase was varied randomly for each frequency of stimulation, and results of ten simulations were averaged.

"Jumping" random grating stimuli

Stimuli that "jumped" suddenly were generated to compare with data from Coombe et al. (1989). These stimuli were spatially random along the preferred-null axis of the EMD array, and uniform in the other dimension. An intensity value for each row of the image was chosen randomly between 0 and 1. The stimulus was spatially shifted by one image pixel (one half of the simulated interommatidial angle) between one timestep and the next, first in the null direction and then in the preferred direction. Data shown are averaged over 100 stimulus presentations, each with a different random grating stimulus.

Results

Even making use of all available anatomical, electrophysiological, and histological data about insect elementary motion detection, there is still not enough information to completely constrain a neuronally based computational model. Thus, for each cell our strategy has been to adopt the *simplest model* which still allows us to demonstrate direction-selective properties at the T5 level. The authors realize that many more details than we have incorporated are known about some cells in the model (particularly about photoreceptors and lamina monopolar cells), but we have included only the essential aspects of each cell in order to keep the model as simple as possible. Up to the Tm1 level, we do not try to model individual synapses, but rather give mathematically relevant expressions for the relationships between cellular responses. While the time constants of filters and the amplitudes of signals in the model were scaled for a close qualitative match with physiological data (e.g. Fig. 6), the model is at a level of abstraction that cannot be expected to reproduce the detailed biophysics of each cell, but rather the outline of their response properties.

The neuronally based EMD model

A block diagram of the model is shown in Fig. 3a. Fig. 5 illustrates the response of each unit in the model to a sinusoidal grating stimulus.

Model photoreceptors respond linearly to the local image intensity. Neural superposition (Nilsson, 1989) is neither explicitly modeled nor required.

The L2 cell, which gets input directly from the photoreceptor and responds to a transient increasing input with a decreasing output, is modeled with a negative high-pass filter. Although this cell is known to have a bandpass temporal-frequency characteristic (Laughlin, 1984; Coombe et al., 1989), the high-frequency cutoff of our model is dominated by low-pass filters in downstream stages, so for L2 we model only the low-frequency response.

Since recent recordings from amacrine cells (Douglass & Strausfeld, 2004) show strong responses across a wide range of frequencies, an amacrine cell in the model responds identically to the photoreceptor in the same optic cartridge. However, since amacrine cells form an input to T1, which exhibits a small response to sustained illumination and an inverted response to light intensity

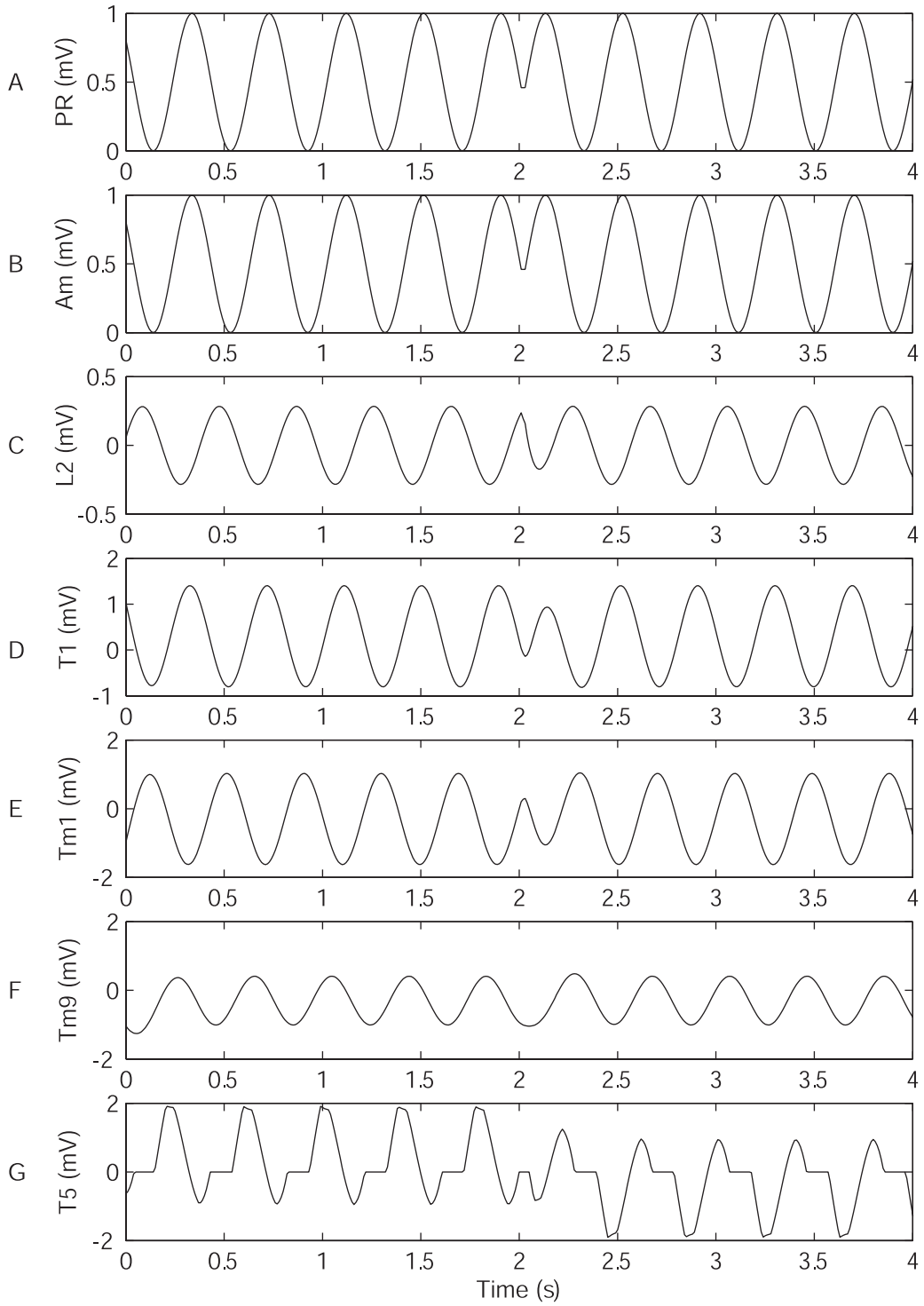

Fig. 5. Responses of neurons in the same model optic cartridge to a moving sinusoidal grating stimulus. The stimulus moves in the preferred direction for 2 s, and then changes to the null direction. Panel A shows the photoreceptor response, changing sinusoidally in correspondence with local luminance. Panel B shows the amacrine unit response, identical to the photoreceptor. Panel C shows the L2 unit, which is sign inverted and high-pass filtered. Note the phase lead relative to the photoreceptor introduced by the high-pass filtering operation. Panel D shows the T1 unit resulting from a combination of six neighboring amacrine units, the synapses of which incorporate a high-pass filter with a small inverted response to mean illumination. The phase of this signal results from the delayed combination of these neighboring units. Panel E shows the Tm1 unit, also incorporating a small response to mean luminance. Panel F shows the Tm9 unit, low-pass filtered (and thus delayed) relative to Tm1. Panel G shows a directionally selective T5 unit which combines the Tm1 and Tm9 units shown with neighboring Tm units to compute the direction of stimulus motion.

(Douglass & Strausfeld, 2004), it is necessary for the amacrine outputs to be high-pass filtered and sign-inverted on the way to T1. These operations are proposed to occur at the amacrine-T1 synapse. The high-pass filtering requirement at the amacrine-T1 synapse is slightly relaxed to allow a small component of sustained response. The surround of amacrine cell outputs summed into each T1 cell is symmetric, taken from all six neighboring optic cartridges. The one-dimensional version of the model shown in Fig. 3a shows a summation of amacrine outputs from left and right neighbors only.

Since the signal from the amacrine cell is relayed through T1 *en route* to Tm1, relative to the L2 cell the amacrine-derived signals in T1 may incur a longer delay to reach Tm1. We model this delay with the phase delay of a LPF placed in the path of each amacrine cell. The T1 cell, which integrates inputs from a surround of six amacrines, may then be modeled simply as a summation. This response is consistent with previously published recordings from T1 (Järvilehto & Zettler, 1973; Douglass & Strausfeld, 1995), which show response properties quite similar to the large monopolar cells in the lamina.

Tm1 is a candidate *nondirectional motion* unit because its anatomical connections allow it to compare the signal from the current optic cartridge provided by L2 with the delayed conglomerate response of surrounding optic cartridges provided by T1. This arrangement makes it possible for Tm1 to detect motion, but not to detect which of the neighboring optic cartridges were stimulated. The model response to flicker (Fig. 6) compares well with the cellular response to similar stimuli. The model response to motion (Fig. 7) is roughly consistent with the recordings available of Tm1. We are not able to support the weak frequency doubling observed by Douglass and Strausfeld (1995) in our current model, and thus our model Tm1 cell shows oscillations at the frequency of stimulation for all directions of motion.

Computationally, the model Tm1 cell represents nondirectional motion in its amplitude (see Appendix for a specific formulation for sinusoidal grating stimuli). Fig. 8 shows how the amplitude of model Tm1 oscillations varies with spatial and temporal frequency. Tm1 is tuned to low spatial frequencies because the sum over space is maximized when the relative phase difference between its inputs is small. The bandpass temporal-frequency response is the result of the high-pass filters interposed in every signal pathway combined with the LPF delays from neighbors. Because the response to full-field flicker (zero spatial frequency) is so strong, the response of this cell may be distinguished from cells such as L2 only by its bandpass spatio-temporal frequency response. However, if responses from an *oriented* surround of amacrine cells were integrated by a T1 cell rather than all six neighbors, then Tm1 could acquire an orientation preference (see Fig. 9) which would enhance responses to edges perpendicular to the directional preference of T5, thus improving its sensitivity to such edges and reducing the effects of the aperture problem (Hildreth & Koch, 1987).

To compute directional motion from Tm cells, T5 cells in our model integrate inputs from an oriented surround of Tm cells in neighboring optic cartridges; that is, T5 integrates inputs from a set of Tm cells that are aligned along one of the two axes of the compound eye (Stavenga, 1979). The simplest version of the model is illustrated in Fig. 3a, in which T5 integrates only inputs

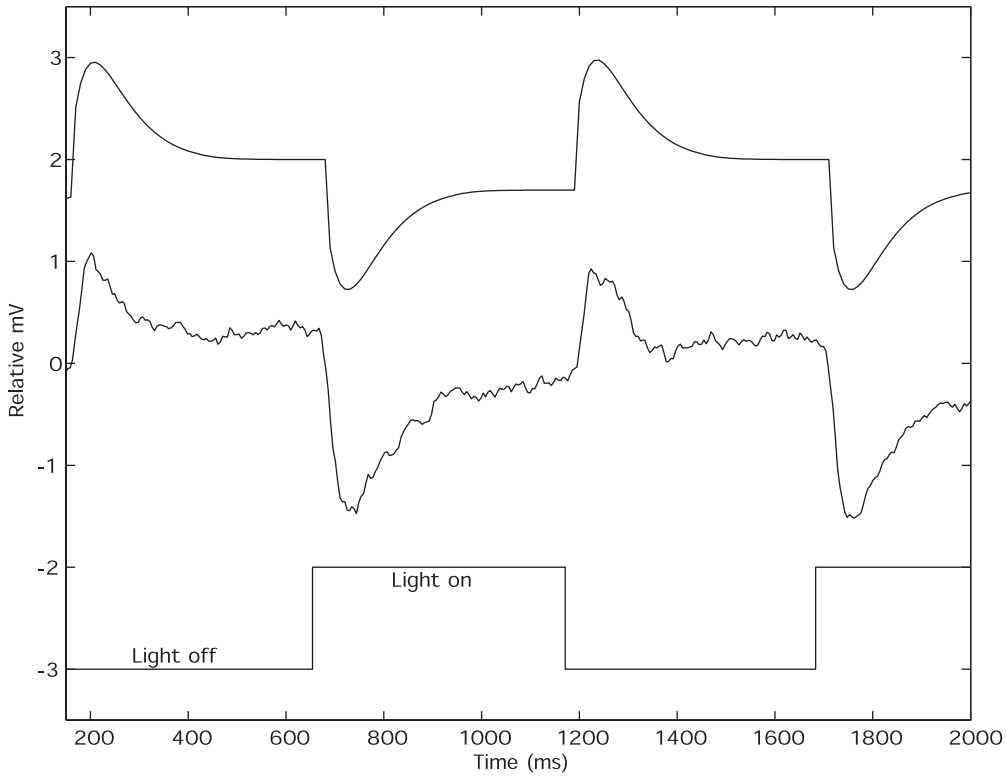

Fig. 6. Intracellular recordings (Douglass & Strausfeld, 1995) from the Tm1 cell (middle trace) in response to full-field square-wave flicker, compared to model response (offset at top). Bottom trace shows light on/off. Cellular response is not unlike a high-pass filter, and compares well with model data.

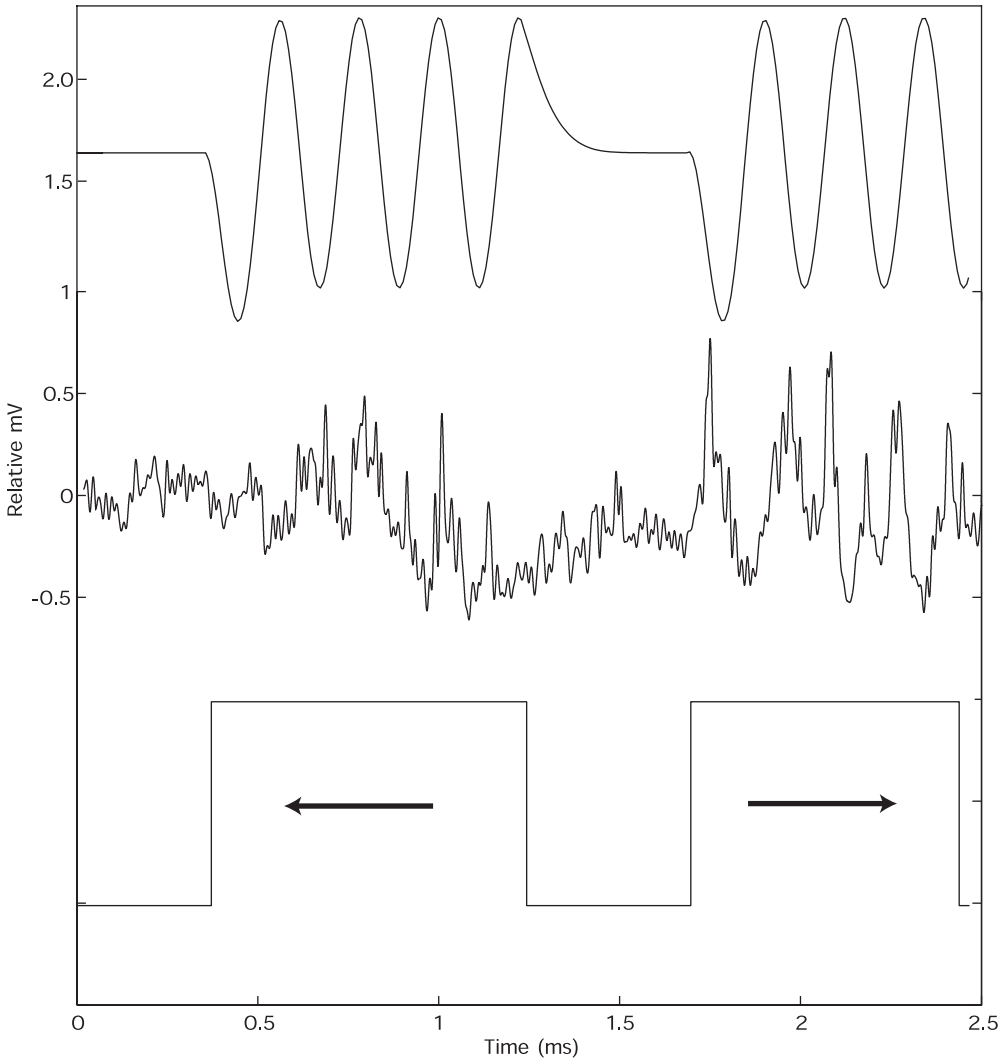

Fig. 7. Response of actual and model Tm1 cells to a moving grating. The center trace shows an electrophysiological recording from the Tm1 cell (Douglass & Strausfeld, 1995). As illustrated in the bottom trace, the initially stationary stimulus moved left, stopped, and then moved right. The top trace shows the Tm1 model response (offset for display). The model cell simply responds at the pattern frequency, independent of direction.

from the Tm cells from the local optic cartridge, and the Tm cells from a neighboring optic cartridge. The model is easily extended to include more Tm inputs by connecting more units in the same manner as the illustrated units.

Because it is the relative timing of the activation of Tm1 units along a particular orientation in retinotopic space which leads to a T5 directional output, and especially in light of recent work in vertebrate retinal directional selectivity (Sterling, 2002; Fried et al., 2002), one is naturally led to think of the model that was proposed by Barlow and Levick (1965) for directional selectivity in the rabbit retina. In the Barlow-Levick (BL) model, direction-selective visual motion units are synthesized by combining excitation from one photoreceptor with delayed inhibition from the neighboring photoreceptor. In this way, if a stimulus passes the excitatory photoreceptor first, the direction-selective cell fires since excitation arrives before inhibition. Conversely, if the inhibitory photoreceptor is stimulated first, inhibition arrives before excitation and the direction-selective cell does not fire.

By making use of the two Tm neurons, Tm1 and Tm9, and realizing that the dendrites of a T5 cell span several optic cartridges, it is possible to support the use of a BL model to synthesize T5 direction selectivity. Tm1 is believed to make an excitatory synapse onto T5 cells (Sinakevitch & Strausfeld, 2004). Tm9 is proposed to receive inputs from Tm1, and to be inhibitory. This pathway is represented in the model by inhibition delayed with a low-pass filter. By making the assumption that each T5 selectively integrates inputs from Tm neurons, it is possible to synthesize a version of the BL model. Since there are four T5 units in every optic cartridge (Strausfeld & Lee, 1991), we propose that two are selective for horizontal motion with opposite preferred directions and two for vertical motion, where horizontal and vertical are defined with respect to the axes of the compound eye (Stavenga, 1979). In order for the mean of the T5 model output to represent direction a nonlinearity is essential (since all input signals are zero-mean), and this can be accomplished if the Tm9 inhibitory input is shunting (see Methods for details of implementation). Shunting inhibition has often been implicated in discussions of the biophysical basis of direction selectivity (Torre & Poggio, 1978; Koch et al., 1982), particularly in those using the BL model. These interconnections serve to make each T5 cell more sensitive to

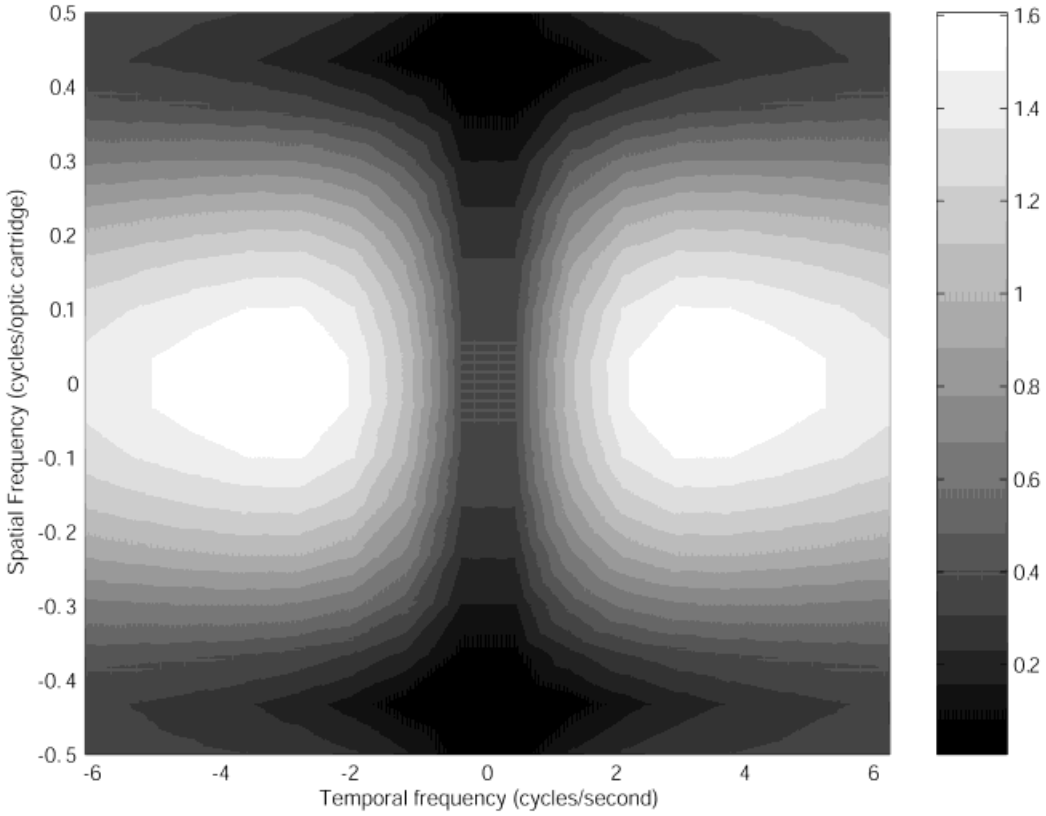

Fig. 8. Amplitude of Tm1 model oscillations as a function of the spatial and temporal frequency of moving sinusoidal gratings. All gratings were moved along the preferred direction axis of the simulated T5 unit. Lighter shading indicates stronger responses, as shown by the scale bar at right. While the response is nondirectional (that is, symmetric on the temporal-frequency axis), it is tuned in both spatial and temporal frequency.

motion in a particular direction, but with strictly positive output sign. Additionally required to make each T5 unit fully directionally selective is an inhibitory interneuron, identified in a recent histological study (Sinakevitch & Strausfeld, 2004), which in our model receives the same inputs as the two T5 cells with the same orientation and provides inhibition to both (see Methods). The temporal response of this model is shown in Fig. 10 and is clearly direction selective in the mean. A theoretical analysis of this algorithm for sinusoidal grating stimuli (in the Appendix) shows that it produces a mean output proportional to the sine of the relative phase of the Tm1 inputs.

The work of Franceschini et al. (1989) suggests an important requirement of this model. Using successive stimulation of adjacent visual sampling units, and recording from the H1 motion-sensitive tangential neuron, the authors showed that elementary motion detectors appear to separate “on” and “off” transient changes in contrast and correlate them separately. This implies that, at some stage in the model, a rectification must be incorporated. Such a rectification follows naturally from the shunting inhibitory connection in the present model. Due to the sign changes inherent in every pathway to the Tm cells combined with our implementation of shunting inhibition [eqn. (3)], the T5 model unit as presented responds only to transiently decreasing intensities. The companion motion detector suggested by Franceschini et al. can be obtained by sign inverting the signals at the Tm outputs relative to their resting potential. Since changing the edge sensitivity of the model only requires sign inversion of the transmedullary outputs, it may well be that two populations of Tm cells coexist to subserve simultaneous correlation of both edges.

To compare the response of the neuronally based EMD model to the HR model, it is necessary to also incorporate into the HR model the rectifying step discussed above. We do this as suggested by Franceschini et al., by inserting a rectifying element after the HPF stage. To match the shape of the temporal-frequency tuning of the neuronally based EMD model, the HR model must use a second-order LPF with poles at the frequencies of the two LPFs used in the neuronally based EMD model (see Appendix). To match the spatial-frequency tuning of the neuronally based EMD model, it is necessary first for the spatial phase difference between the photoreceptor inputs used in the HR model to equate to a single optic cartridge, as in the neuronally based EMD model. In addition, it is necessary to match the spatial width of the neuronally based EMD model by averaging inputs from three neighboring photoreceptors as shown in Fig. 3b.

Under these conditions, despite their considerable differences, the outputs of the two models are quite comparable. The response of the neuronally based EMD model is compared to electrophysiological recordings from T5 and to the HR model in Fig. 10 and although, as expected, it does not reproduce the detailed biophysical properties of the cell, it is in good qualitative agreement with both the cellular data and the HR model (see Discussion). The mean response to sinusoidal grating stimuli of the neuronally based EMD model is compared to the HR model in Fig. 11. Like all biological elementary motion detectors, both models exhibit

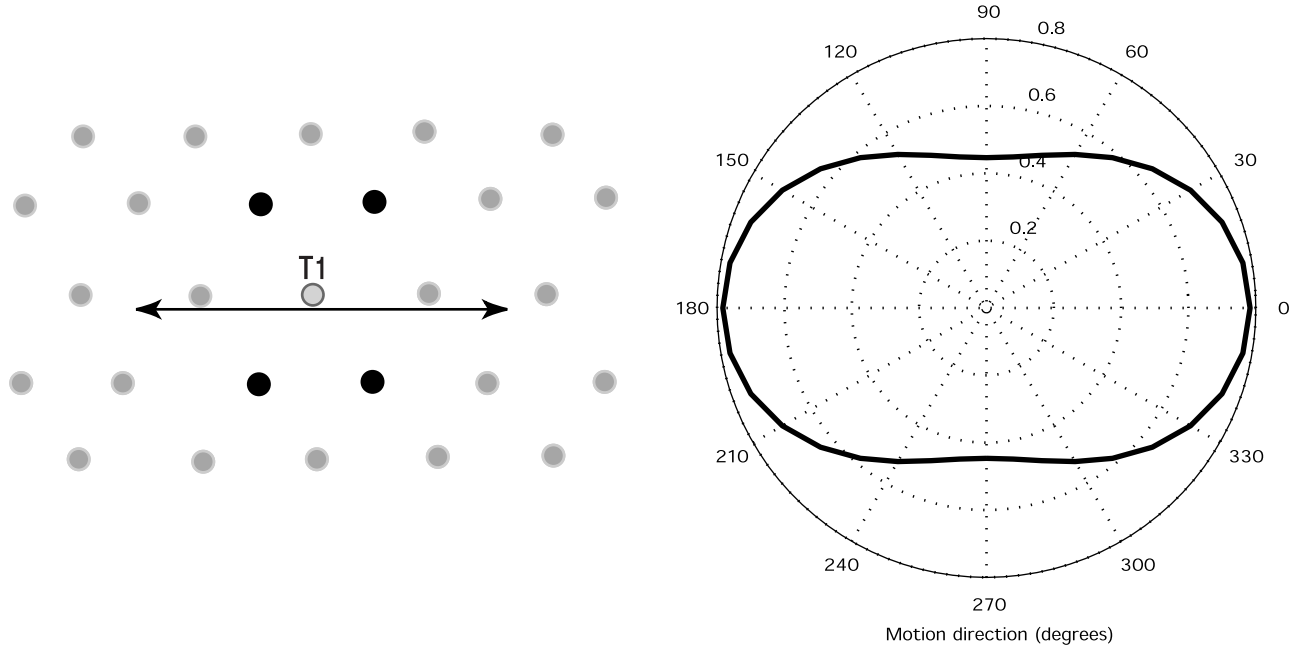

(a) (b)

Fig. 9. Orientation-selective Tm1 unit. Tm1 can be given an orientation preference by integrating inputs from a select surround of amacrine cells. (a) If the T1 (and thus Tm1) unit in the center optic cartridge integrates amacrine inputs from the selected neighboring optic cartridges marked in black, it will be more sensitive to stimulus orientations along the axis of the T5 preferred-null directions (arrowed line). (b) Resulting orientation preference of Tm1. The preferred direction of the corresponding T5 cell is 0 deg.

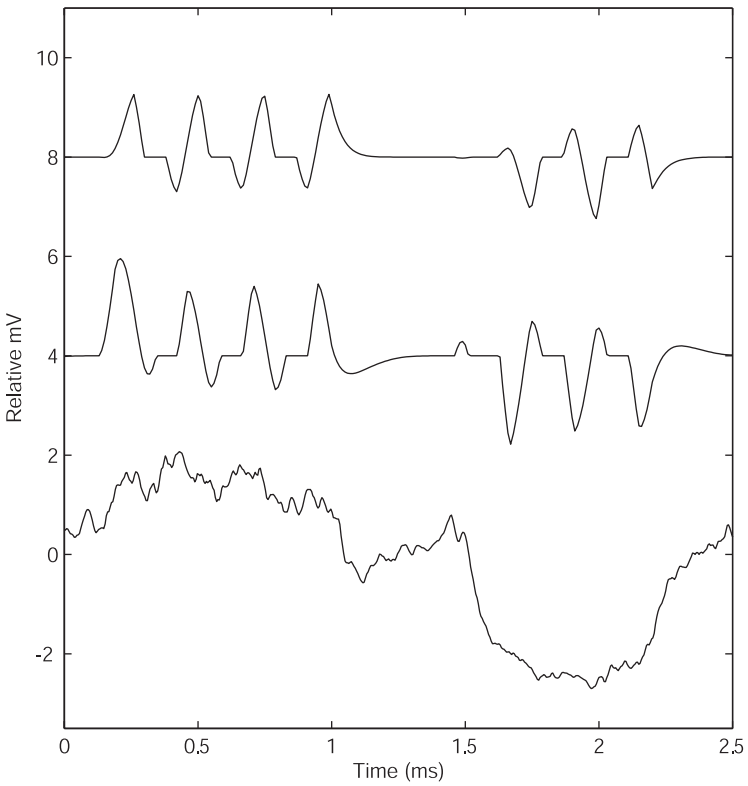

Fig. 10. Comparison of motion responses of HR model (top trace), neuronally based EMD model (middle trace), and electrophysiological data recorded from a T5 cell (bottom trace, from Douglass & Strausfeld, 1995). The stimulus was a grating that moved to the left for 1 s, stopped for 0.5 s, and then moved to the right. While the detailed biophysics of T5 are clearly not predicted by the models, the general response properties of all three traces are similar (see Discussion).

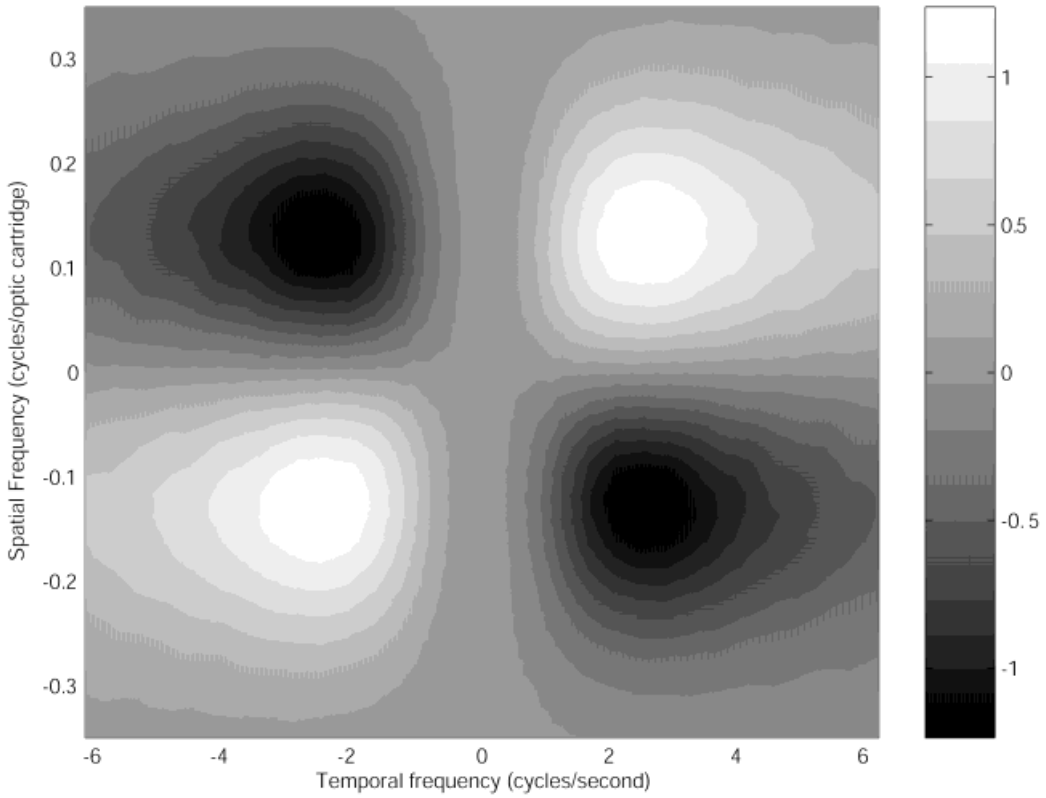

(a)

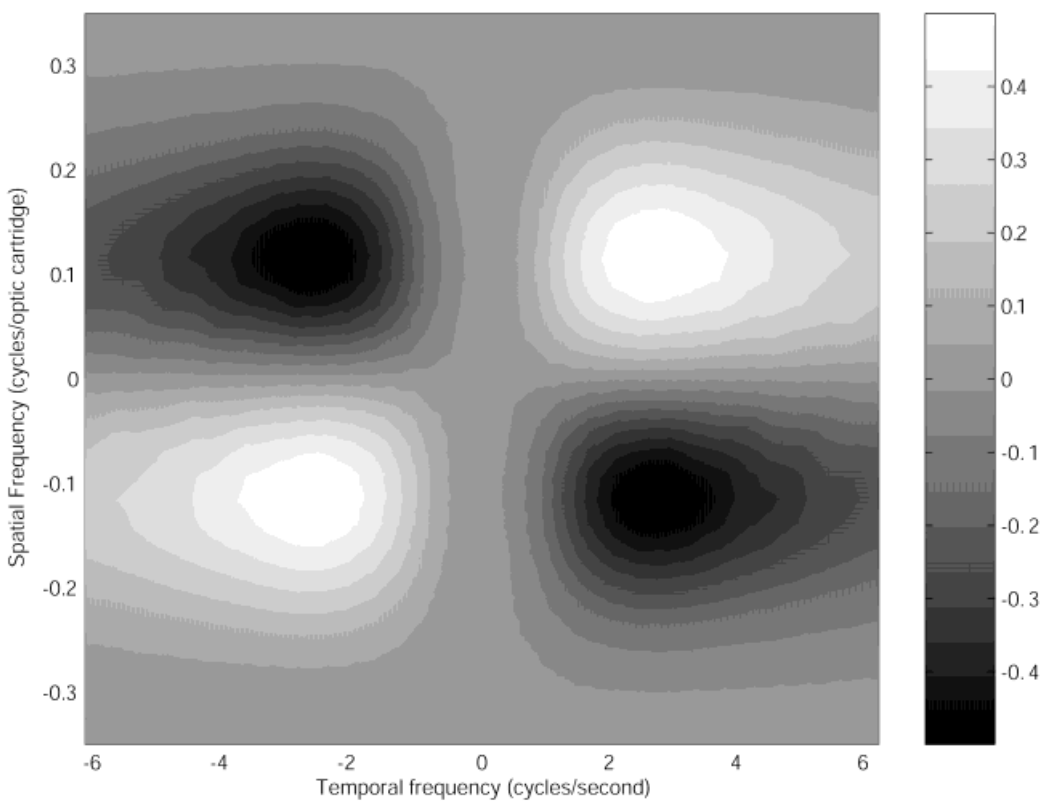

(b)

Fig. 11. Mean response of model EMDs to simulated sinusoidal gratings of varying spatial and temporal frequency. (a) Neuronally based EMD model. (b) HR model. Lighter shading indicates stronger responses, as shown by the scale bars at right. Both models are spatial and temporal frequency tuned, and show very similar tunings.

bandpass tuning in spatial and temporal frequency, rather than sensitivity to stimulus velocity without regard to spectral content. The choice of parameters in the HR model (see Methods) produces approximately the same spectral shape as the neuronally based EMD model.

Comparison with predictions from tangential cells

Most of the experiments which have been performed to elucidate the nature of elementary motion detection (Franceschini et al., 1989; Coombe et al., 1989; Egelhaaf & Borst, 1989) have involved presentation of transient (aperiodic) visual stimuli while performing electrophysiological recordings from lobula plate tangential cells, which are believed to spatially integrate outputs from multiple EMDs. Versions of the HR model have been used to successfully predict tangential cell responses in most of these experiments. Although the novel neuronally based EMD model and the canonical HR model show very similar mean responses to drifting sinusoidal visual stimuli (see Appendix), neither model is mathematically a linear system, nor are the models equivalent, and thus it is not obvious that transient responses of the neuronally based EMD model to complex stimuli must agree with the HR model.

All of the neurons discussed in the model so far represent their activity in a graded membrane potential. However, many tangential cells, including the well-studied H1 horizontal cell (Franceschini et al., Coombe, et al., 1989), are *spiking* neurons; that is, they represent their activation in a train of action potentials. For this reason, many tangential cells exhibit a rectifying characteristic, responding with an increase in firing frequency to stimuli in the preferred direction but often exhibiting only inhibition of the spontaneous firing rate in response to null-direction stimuli.

For these reasons, to test the present model against the vast majority of experimental predictions about EMDs, we must spatially integrate our model outputs over multiple optic cartridges to synthesize a generic model tangential cell, the output of which represents mean firing rate (see Methods for details). Because the actual magnitude of responses from the generic tangential cell model is not comparable to a specific tangential cell, most responses are presented in normalized form.

A qualitative, but not quantitative, match of our model to electrophysiological data from lobula plate tangential cells is to be expected for several reasons. Firstly, as many parameters of our model as possible are tuned to electrophysiologically measured properties of specific lamina and medulla neurons, but it is quite conceivable that multiple tunings may exist in the insect among morphologically similar types of neurons. Secondly, adaptation is well known to exist in the neurons of insect optic lobes (Maddess & Lauhhlin, 1985; de Ruyter van Steveninck et al., 1997; Harris et al., 1999; O'Carroll, 2001) and is not addressed in the present model. Such adaptation can alter the temporal response of a tangential cell as a stimulus continues, and make present responses dependent on past stimuli. Neither effect will be predicted by the present model. Finally, our simple wide-field neuron model integrates inputs from a large number of identical cells without regard to the specific tuning properties of the wide-field cell being modeled. However, a qualitative match goes far to prove plausibility of the model and may suggest electrophysiological experiments to validate the present model as opposed to the HR model.

Response to impulses and steps

The experiments of Franceschini et al. (1989) demonstrated a number of features of elementary motion detection, all of which are also exhibited by the present model. First, there was no significant response to flash stimulation of either photoreceptor alone, a fact predicted easily by the HR model by virtue of the fact that either pathway having zero activation multiplies the response of the other pathway by zero. This is *not* true in the present model of elementary motion detection. In fact, in response to stimulation of a single photoreceptor, a number of our model EMDs respond as shown in Fig. 12 (although weakly, compared to their response to motion). However, because their response is spatially symmetric and the tangential cell reflects a spatial sum, the flash response of our simulated tangential cell is extremely small relative to its response to motion stimuli, as predicted by the experimental data.

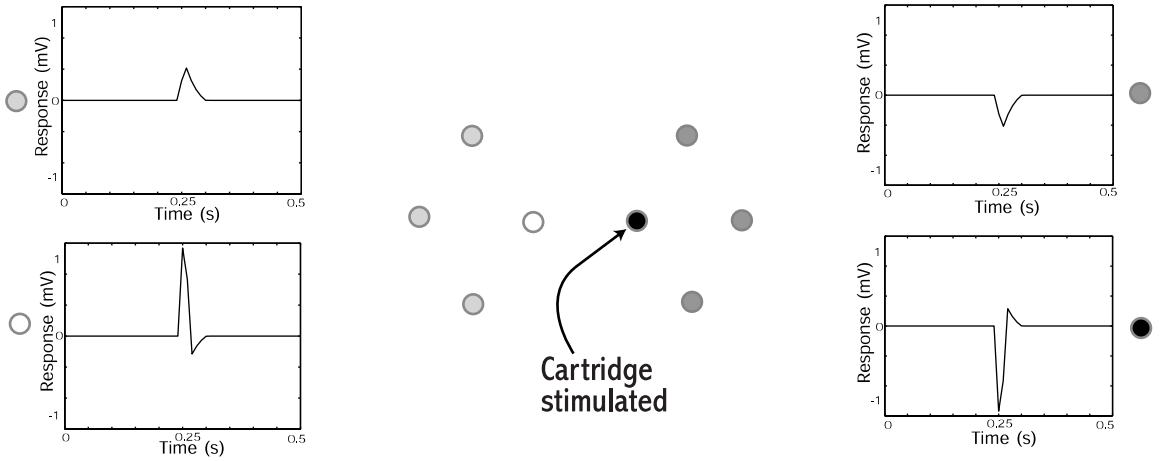

Fig. 12. Responses of model T5 cells to flash stimulation of a single photoreceptor. Four classes of T5 responses are observed, represented by black, light gray, dark gray, and white circles. The graphs at left and right show the four classes of temporal responses, and the diagram at center shows the spatial pattern of these activations relative to the stimulated optic cartridge. A short (10-ms) flash stimulus was applied to the photoreceptor in a single optic cartridge (black circle), which responds with a negative output due to spatially imbalanced inputs. Surrounding T5 cells respond as shown. Optic cartridges not shown have no response. While multiple T5 units respond, in spatial sum the overall response is zero.

Franceschini et al. also showed that there was no response of the tangential cell to synchronous flash stimulation of both photoreceptors. This is in agreement with the HR model due to the balanced nature of the two subunits and the subtraction at its output. Similar to the result with single-photoreceptor stimulation described above, while individual T5 model units *do* respond to this stimulus, the spatial sum remains very close to zero.

Crucially, the Franceschini et al. experiment showed that the H1 cell responded in a direction-selective manner to sequential flash stimulation of two neighboring photoreceptors. The T5-based generic tangential cell model response, shown in Fig. 13a, provides a good qualitative match to the cellular response from Franceschini et al. (1989). Qualitatively similar results are obtained using the HR model.

Two further highly revealing predictions resulted from this series of experiments. Firstly, by plotting the peak firing rate of the H1 cell as the time between flash stimuli at the two adjacent optic cartridges was varied, a curve was generated which started at zero for simultaneous flashes and returned to zero for very long inter-flash times. Franceschini et al., working on the basis of the HR model, believed that this response represented the "facilitatory control" represented by the LPF in the HR model. The response that they obtained looked like the impulse response of a higher-order low-pass filter. The response of the present model to this pattern of stimulation is shown in Fig. 13b, and shows a good qualitative match with the experimental data. Secondly, by turning on sustained illumination to one photoreceptor and later the neighbor, they were able to show the step response of the "direct path", which they believed to be a high-pass filter. The response of the T5-based tangential cell model to an analogous stimulus is shown in Fig. 13c and shows a good match to the experimental data.

Transient responses to moving sinusoidal gratings

To allow comparison of the response of our model to the experimental data of Egelhaaf and Borst (1989), we have performed simulations of our T5-based generic tangential cell model with transiently moving sinusoidal visual stimuli and compared them to the response of an HR-based generic tangential cell model

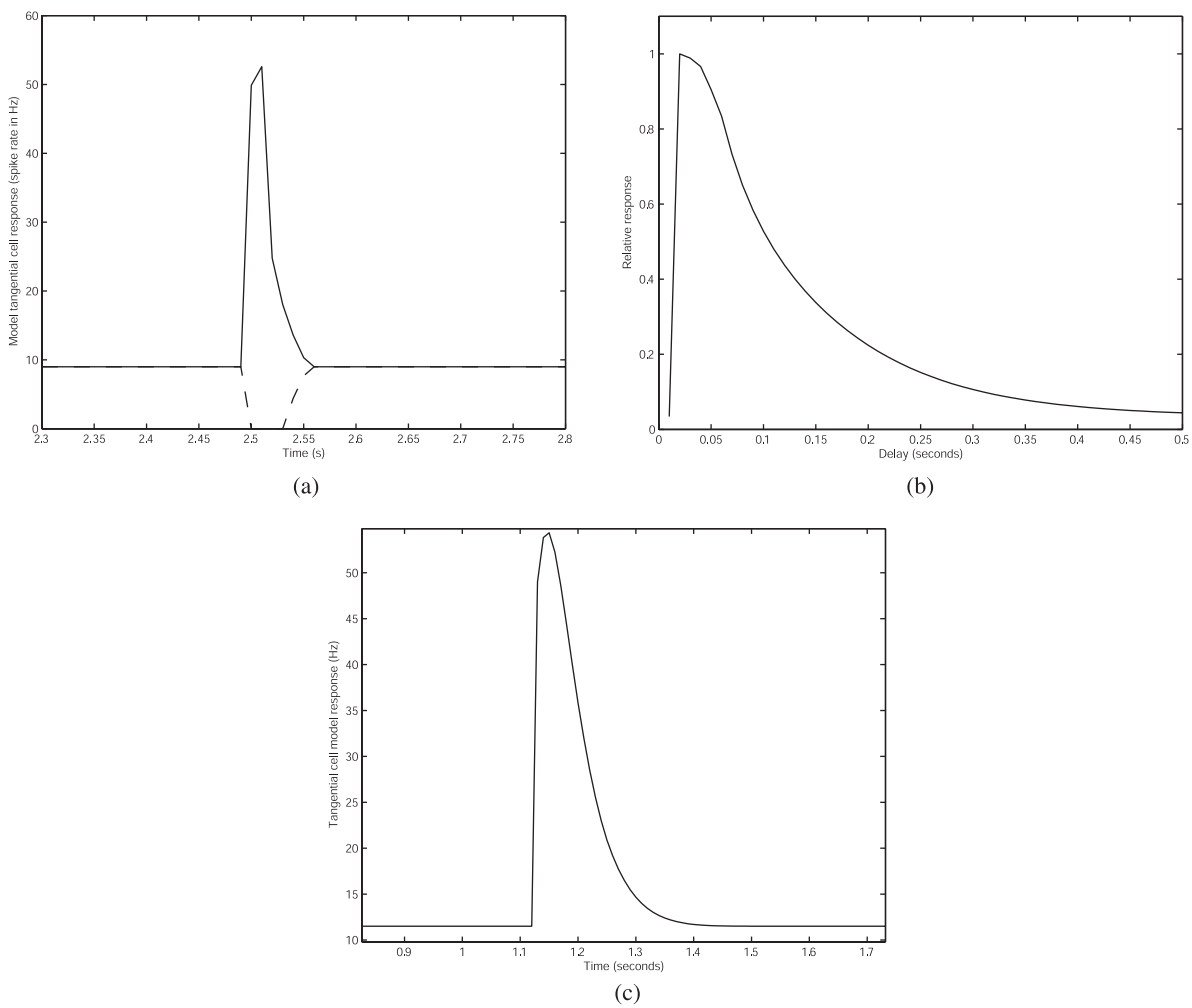

Fig. 13. Responses of model generic tangential cell to flash and step stimuli similar to those employed by Franceschini et al. (1989). (a) Response to sequential flash stimulation of two neighboring photoreceptors. The preferred-direction response is shown as a solid line, and the null-direction response as a dashed line. (b) Effect of varying the interval between sequential flash stimulation of two neighboring photoreceptors. The trace shows a shape that is comparable to the impulse response of a low-pass filter. (c) Response to a sustained intensity step at one photoreceptor followed 100 ms later by a step at the next. The step was applied to the first photoreceptor at 1 s, and to the next at 1.1 s. This response is comparable to the step response of a high-pass filter.

to identical stimuli in Fig. 14. Since the HS tangential cell data collected by Egelhaaf and Borst were intracellular subthreshold membrane potentials, for this data the spontaneous firing rate offset and rectification stages are not employed in the generic tangential cell model. The transient oscillations show a good match between the two models. In both models, the oscillation is at the frequency of the sinusoidal grating, and is due to transient responses of high-pass and low-pass filters in the computation.

Response to "jumping" stimuli

Coombe et al. (1989) presented an H1 tangential cell with saltatory (suddenly "jumping") random gratings and observed a direction-selective (although very weak) response. On the basis of this evidence, they argued that it is not possible for all inputs to the insect EMD to be high-pass filtered. High-pass filters discard the tonic portion of the signal, and the EMD must retain some memory of the static pattern being presented in order to respond directionally to saltatory gratings. Coombe et al. further showed electrophysiologically that LMCs have no sustained response to illumination, and therefore cannot alone provide all inputs to the EMD. Indeed, while it responds readily to smoothly moving gratings, it is quite impossible for the HR motion detection model as formulated here to respond directionally to saltatory gratings, due to having only high-pass filtered inputs. If the jump is small enough, it will stimulate changes in only a single optic cartridge which is input to a given EMD, and we have already discussed that the HR model does not respond to this stimulus.

The neuronally based EMD model, however, has one input pathway (through the amacrine-T1 synapse) which allows a small sustained response component (see Methods). With this pathway, a predictable but very weak response to saltatory gratings similar to those used in Coombe et al. (1989) is seen (averaged over 100 stimulus presentations) in the T5-based model tangential cell (Fig. 15).

Discussion

We have described and evaluated a novel model of elementary motion detection in the fly. The responses of this model were shown to be comparable to those of the canonical HR model, and in close qualitative agreement with previous predictions of EMD properties. The HR model does not, and was never intended to, reflect real neuronal arrangements. The present model of elementary motion detection is the first which derives specifically from the functional organization of a subset of retinotopic neurons supplying the lobula plate. This subset is not unique to the fly, but has been recognized across insect taxa. Its cellular counterparts in other arthropods suggest an ancient origin for this circuit and, thus, in modern taxa, a fine tuning that has resulted from hundreds of millions of years of evolutionary refinement.

Much of this paper is devoted to demonstrating that the neuronally based EMD model has output properties that are close to those of the canonical HR model. Thus, while the present EMD model is consistent with the anatomical and physiological observations of real neurons, it can be argued that it does not contribute to any further understanding of lobula plate tangential cell responses, as these can be satisfactorily predicted by notional HR inputs. What value, then, does the neuronally based EMD model add? Firstly, a key prediction of the present model is that individual EMDs, while direction selective, respond quite differently to

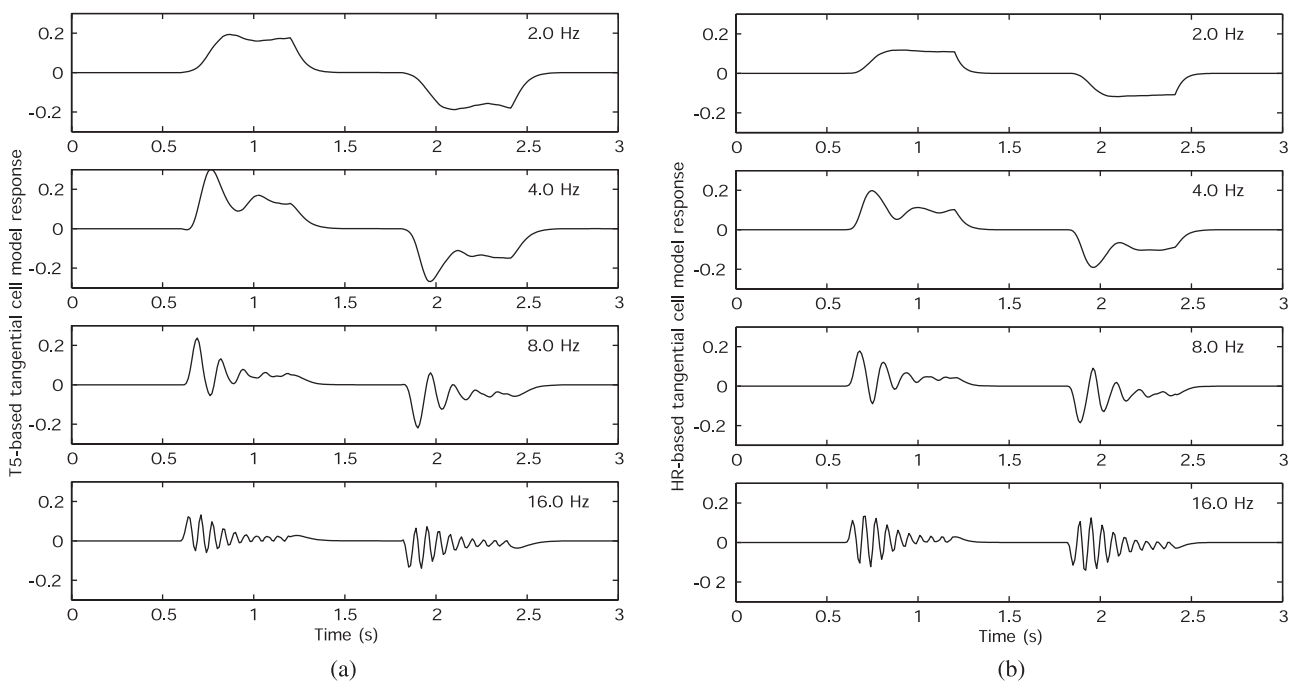

Fig. 14. Transient responses of generic tangential cell models to sinusoidal gratings across a range of temporal frequencies. (a) Responses of T5-based tangential cell model. (b) Responses of comparable HR-based tangential cell model. Each grating stimulus had optimal orientation and spatial frequency. The stimulus was stationary for 0.6 s, moved the left for 0.6 s, was stationary again for 0.6 s, and then moved the right for 0.6 s. Responses shown are the average of ten simulations each started with a random spatial phase. Both models show comparable transient oscillations at the pattern temporal frequency.

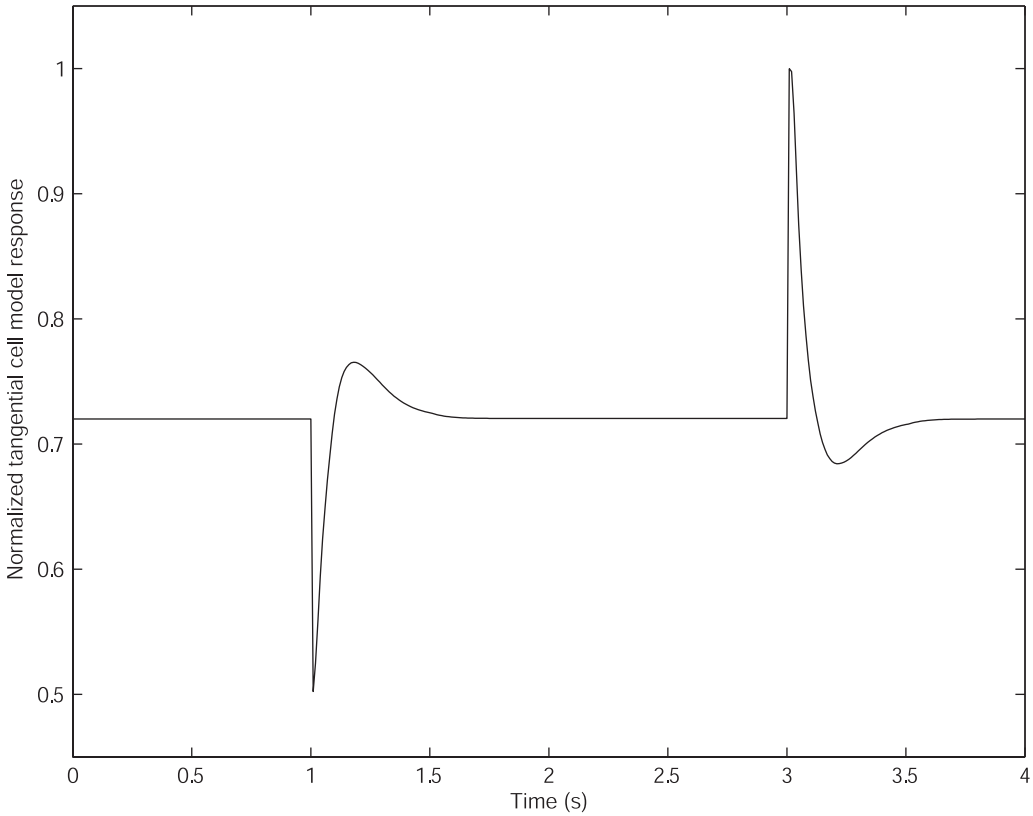

Fig. 15. Normalized mean response of T5-based generic tangential cell to a static random grating (see Methods for details) which "jumps" suddenly in the null direction at 1 s, then in the preferred direction at 3 s. The response is clearly direction-selective.

small-field transient stimulation than do spatially integrated EMDs as observed in the lobula plate. This fact is completely unexpected from the HR model, which in very similar forms is used as a model of an EMD or a tangential cell, and is, at least in principle, experimentally testable. Secondly, while T5 cells from the outer layer of the lobula supply inputs to lobula plate tangential cells, there is no evidence that they also supply inputs to motion-sensitive tangential neurons elsewhere in the optic lobes. The best known examples of such neurons are from studies of male flies in which, depending on the cell type, wide-field lobula neurons subtending the upper frontal visual field have directionally selective responses to small- or wide-field motion (Gilbert & Strausfeld, 1991). Such cells must play crucial roles in target perception and pursuit, behaviors that critically depend on motion computation (Collet & Land, 1978). How, then, would such neurons be supplied with motion information? One answer is suggested by the present model, which reconstructs motion in several stages. The neuronally based EMD circuit could provide a collateral supply to the lobula if this were derived from the circuit at the level of Tm cells. Such collateral channels would be mediated by parallel Tm cells to deeper levels in the lobula. This supply cannot be emulated by the HR model, which is missing the intermediate stages of processing represented by the activity of Tm cells. This may be the most important reason to further develop the neuronally based EMD model: it will allow a unified approach to computational modeling of a wide range of visually guided behaviors, not just those represented by large cells in the lobula plate.

Especially since the *responses* of the neuronally based EMD model are so similar to both the HR (Van Santen & Sperling, 1985) and Adelson-Bergen (Adelson & Bergen, 1985) models, it is tempting to try to fit this model into the existing theoretical framework. In fact, the Barlow-Levick model used in the Tm1–T5 stage is quite closely related to the other spatio-temporal frequency tuned motion detection models (Ibbotson, 2001; Clifford & Ibbotson, 2003), and if one simplifies the shunting inhibition "dirty multiplication" to a real multiplication, the model from Tm1 to T5 does actually implement a form of "Reichardt detector." The computation of motion in multiple stages, beginning with a representation of nondirectional motion at the Tm1 stage, and culminating in the computation of directional motion *from nondirectional motion*, is a novel prediction of the present model.

There is strong anatomical evidence that there exist four morphologically similar T5 cells in each optic cartridge (Buchner & Buchner, 1984; Strausfeld & Lee, 1991). Our model suggests a role for each of the four T5 units. Each group of four T5s in a given optic cartridge could represent two roughly orthogonal orientations along the lattice of the compound eye (Stavenga, 1979), each with opposite preferred directions.

Amacrine cells are well described anatomically, and they together comprise an isomorphic assembly across the entire lamina. Distally, they provide a discrete hexagonal network of processes that synapse with each other and which lie completely segregated from deeper synaptic levels associated with photoreceptor terminals. These processes, however, provide long varicose extensions, each equipped with rows of pinhead-like spicules, that extend through the lamina's depth where they run along the outer surfaces of receptor endings. Each of these processes is paired with a similarly shaped ascending process belonging to a T1 efferent

neuron that carries information from the lamina to the medulla, in parallel with the L2 monopolar cell from the same cartridge. T1 neurons invest single cartridges, whereas amacrine cells provide connections among surrounding cartridges (Campos-Ortega & Strausfeld, 1973). It is very likely that the hexagonal surround of amacrines suggested in the model is oversimplified. More likely is that the amacrine network spreads activity across a number of optic cartridges. If so, this could provide a method of controlling the spatial-frequency response of each EMD: the larger the surround of amacrines involved in synthesizing the responses of each Tm1 cell, the lower the optimal spatial frequency. The optimal temporal frequency tuning of the model can be changed simply by varying time constants of the temporal filters.

While we have modeled the output of a Tm1 unit from two neighboring optic cartridges being integrated by each T5 cell, a number of Tm1 outputs in an oriented spatial pattern can be summed into each T5 unit without changing the direction-selective properties. Summing outputs from additional optic cartridges would certainly increase the sensitivity of the T5 unit to low contrast, but would also reduce sensitivity to high spatial frequencies.

A number of causes already mentioned could be responsible for the stronger stimulus phase dependence shown by the simulated T5 unit in Fig. 10 relative to the T5 neural recording. Amacrine cells receiving inputs from a network of photoreceptors could reduce phase dependence by integrating inputs across multiple optic cartridges. T5 units integrating a larger number of oriented Tm1 outputs would have much the same effect.

While the response of the present model does not saturate with contrast in the way that H1 cells do (Egelhaaf & Borst, 1989), neither does the HR model as shown. Egelhaaf and Borst (1989) suggested the addition of saturating elements into each input pathway of the HR model, and the same mechanism can be used in the present model to obtain contrast saturation (Rivera-Alvidrez & Higgins, 2004).

It is rarely seen in electrophysiological data that a direction-selective neuron has such perfectly balanced responses to preferred- and null-direction motion as the neuronally based EMD model exhibits in Fig. 10. In the HR model, the gain between "subunits" is often varied to better match experimental data (Egelhaaf et al., 1989). A similar balance between the strength of preferred- and null-direction responses can be found in the neuronally based EMD model by varying the parameter a in eqn. (4). As a is varied up or down from its nominal value of 0.5, the strength of response in one stimulus direction is lessened with respect to the other.

Acknowledgments

The authors were supported by the U. S. Air Force Office of Scientific Research through STTR contract number SC-25627-1374-03 to Physical Sciences, Inc. (Andover, MA). N.J. Strausfeld and J.K. Douglass were also supported by grant number R01 RR08688 from the National Institutes of Health. The authors would like to thank Dr. Alexander Borst of the Max-Planck-Institute of Neurobiology, Martinsreid, Germany for helpful technical correspondence.

References

Adelson, E.H. & Bergen, J.R. (1985). Spatiotemporal energy models for the perception of motion. *Journal of the Optical Society of America A* **2**(2), 284–299.

Barlow, H.B. & Levick, W.R. (1965). The mechanism of directionally selective units in rabbit's retina. *Journal of Physiology (London)* 178, 477–504.

Bausenwein, B. and Fischbach, K.-F. (1992). Separation of functional pathways in the fly's medulla: combination of 2-deoxyglucose studies with anatomical fine analysis. In *Nervous Systems: Principles of Design and Function*, ed. Singh, R.N., pp. 223–239. New Delhi, India: Wiley Eastern.

Borst, A. (2001). Modelling fly motion vision. In *Computational Neuroscience: A Comprehensive Approach*, ed. Feng, Jianfeng, pp. 401–434. Boca Raton, FL: CRC Press.

Borst, A. and Haag, J. (2002). Neural networks in the cockpit of the fly. *Journal of Comparative Physiology A* **188**, 419–437.

Boschek, C.B. (1971). On the fine structure of the peripheral retina and the lamina of the fly, *Musca domestica*. *Zeitschrift für Zellforschung und Mikroskopische Anatomie* **110**, 336–349.

Buchner, E. & Buchner, S. (1984). Neuroanatomical mapping of visually induced neuron activity in insects by 3H-deoxyglucose. In *Photoreception and Vision in Invertebrates*, ed. Ali, M.A., pp. 623–634. New York: Plenum Press.

Buchner, E., Buchner, S., & Hengstenberg, R. (1979). 2-Deoxy-D-glucose maps movement-specific nervous activity in the second visual ganglion of *Drosophila*. *Science* **205**, 687–688.

Buschbeck, E.K. & Strausfeld, N.J. (1996). Visual motion-detection circuits in flies: Small field retinotopic elements responding to motion are evolutionarily conserved across taxa. *Journal of Neuroscience* **16**, 4563–4578.

Campos-Ortega, J.A. & Strausfeld, N.J. (1973). Synaptic connections of intrinsic cells and basket arborizations in the external plexiform layer of the fly's eye. *Brain Research* **59**, 119–136.

Clifford, C.W.G. & Ibbotson, M.R. (2003). Fundamental mechanisms of visual motion detection: Models, cells and functions. *Progress in Neurobiology* **68**, 409–437.

Collett, T.S. & Land, M.F. (1978). How hoverflies compute interception courses. *Journal of Comparative Physiology* **125**, 191–204.

Coombe, P.E., Srinivasan, M.V., & Guy, R.G. (1989). Are the large monopolar cells of the insect lamina on the optomotor pathway? *Journal of Comparative Physiology A* **166**, 23–35.

de Ruyter van Steveninck, R., Lewen, G.D., Strong, S.P., Koberle, R., & Bialek, W. (1997). Reproducibility and variability in neural spike trains. *Science* **275**, 1805–1808.

Douglass, J.K. & Strausfeld, N.J. (1995). Visual motion detection circuits in flies: Peripheral motion computation by identified small field retinotopic neurons. *Journal of Neuroscience* **15**, 5596–5611.

Douglass, J.K. & Strausfeld, N.J. (1996). Visual motion detection circuits in flies: Parallel direction-and non-direction sensitive pathways between the medulla and lobula plate. *Journal of Neuroscience* **16**, 4551–4562.

Douglass, J.K. & Strausfeld, N.J. (1998). Functionally and anatomically segregated visual pathways in the lobula complex of a calliphorid fly. *Journal of Comparative Neurology* 396: 84–104.

Douglass, J.K. & Strausfeld, N.J. (2004). Sign-conserving amacrines in the fly's external plexiform layer. *Visual Neuroscience* (in review).

Dvorak, D.R., Bishop, L.G., & Eckert, H.E. (1975). Intracellular recording and staining of directionally selective motion detecting neurons in fly optic lobe. *Vision Research* **15**, 451–453.

Egelhaaf, M. & Borst, A. (1989). Transient and steady-state response properties of movement detectors. *Journal of the Optical Society of America A* **6**, 116–127.

Egelhaaf, M., Borst, A., & Reichardt, W. (1989). Computational structure of a biological motion-detection system as revealed by local detector analysis in the fly's nervous system. *Journal of the Optical Society of America A* **6**, 1070–1087.

Egelhaaf, M., Borst, A., Warzecha, A.K., Flecks, S., & Wildemann, A. (1993). Neural circuit tuning fly visual neurons to motion of small objects. II. Input organization of inhibitory circuit elements revealed by electrophysiological and optical recording techniques. *Journal of Neurophysiology* **69**, 340–351.

Egelhaaf, M., Hausen, K., Reichardt, W., & Wehrhahn, C. (1988). Visual course control in flies relies on neuronal computation of object and background motion. *Trends in Neuroscience* **11**, 351–358.

Fischbach, K.-F. & Dittrich, A.P.M. (1989). The optic lobe of *Drosophila melanogaster*. I. A Golgi analysis of wild-type structure. *Cell and Tissue Research* **258**, 441–475.

Franceschini, N., Riehle, A., & Le Nestour, A. (1989). Directionally selective motion detection by insect neurons. In *Facets of Vision*, ed. Stavenga, D.G. & Hardie, R.C., chapter 17, pp. 360–390. Springer-Verlag.

Fried, S.I., Münch, T.A., & Werblin, F.S. (2002). Mechanisms and circuitry underlying directional selectivity in the retina. *Nature* **420**, 411–414.
Gilbert, C. & Strausfeld, N.J. (1991). The functional organization of male-specific visual neurons in flies. *Journal of Comparative Physiology A* **169**, 395–411.
Harris, R.A., O'Carroll, D.C., & Laughlin, S.B. (1999). Adaptation and the temporal delay filter of fly motion detectors. *Vision Research* **39**, 2603–2613.
Hassenstein, B. (1950). Wandernde geometrische Interferenzfiguren im Insektenauge. *Naturwissenschaften* **37**, 45–46.
Hassenstein, B. (1951). Ommatidienraster und afferente Bewegungsintegration. *Zeitschrift für vergleichende Physiologie* **33**, 301–326.
Hassenstein, B. (1958). Die Stärke von optokinetschen Reaktionen auf verschiedene Mustergeschwindigkeiten. *Zeitschrift für Naturforschung* **13b**, 1–6.
Hassenstein, B. & Reichardt, W. (1956). Systemtheorische analyse der Zeit-, Reihenfolgen-und Vorzeichenauswertung bei der Bewegungsperzeption des Rüsselkäfers *Chlorophanus*. *Zeitschrift für Naturforschung* **11b**, 513–524.
Hausen, K. (1982). Motion sensitive interneurons in the optomotor system of the fly. I. The horizontal cells: Structure and signals. *Biological Cybernetics* **45**, 143–156.
Hausen, K. (1984). The lobula-complex of the fly: Structure, function, and significance in visual behaviour. In *Photoreception and Vision in Invertebrates*, ed. Ali, M.A., pp. 523–599. New York: Plenum Press.
Hildreth, E.C. & Koch, C. (1987). The analysis of visual-motion-from computational theory to neuronal mechanisms. *Annual Review of Neuroscience* **10**, 477–533.
Ibbotson, M.R. (2001). Identification of mechanisms underlying motion detection in mammals. In *Motion Vision: Computational, Neural, and Ecological Constraints*, ed. Zanker, J.M. & Zeil, J., pp. 57–65. Berlin: Springer.
James, A.C. & Osorio, D. (1996). Characterisation of columnar neurons and visual signal processing in the medulla of the locust optic lobe by system identification techniques. *Journal of Comparative Physiology A* **178**, 183–199.
Järvilehto, M. & Zettler, F. (1973). Electrophysiological-histological studies on some functional properties of visual cells and second-order neurons of an insect retina. *Zeitshchrift für Zellforschung und Mikroskopische Anatomie* **136**, 291–306.
Koch, C. (1999). *Biophysics of Computation: Information Processing in Single Neurons*. New York: Oxford University Press.
Koch, C., Poggio, T., & Torre, V. (1982). Retinal ganglion cells: A functional interpretation of dendritic morphology. *Philosophical Transactions of the Royal Society B* (London) **298**, 227–264.
Krapp, H.G., Hengstenberg, B., & Hengstenberg, R. (1998). Dendritic structure and receptive-field organization of optic flow processing interneurons in the fly. *Journal of Neurophysiology* **79**, 1902–1917.
Laughlin, S (1984). The roles of parallel channels in early visual processing by the arthropod compound eye. In *Photoreception and Vision in Invertebrates*, ed. Ali, M.A., pp. 457–482. New York: Plenum Press.
Maddess, T. & Laughlin, S.B. (1985). Adaptation of the motion sensitive neuron H1 is generated locally and governed by contrast frequency. *Proceedings of the Royal Society B* (London) **225**, 251–275.
Nilsson, D.-E. (1989). Optics and evolution of the compound eye. In *Facets of Vision*, ed. Stavenga, D.G. & Hardie, R.C., Chapter 3, pp. 30–73. Berlin: Springer-Verlag.
O'Carroll, D.C. (2001). Motion adaptation and evidence for parallel processing in the lobula plate of the bee-fly *Bombylius major*. In *Motion Vision: Computational, Neural, and Ecological Constraints*, ed. Zanker, J.M. & Zeil, J., pp. 381–394. Berlin: Springer.
Pix, W., Zanker, J.M., & Zeil, J. (2000). The optomotor response and spatial resolution of the visual system in male *Xenos vesparum (strepsiptera)*. *Journal of Experimental Biology* **203**, 3397–3409.
Reichardt, W., Egelhaaf, M., & Guo, A.K. (1989). Processing of figure and background motion in the visual-system of the fly. *Biological Cybernetics* **61**, 327–345.
Rivera-Alvidrez, Z. & Higgins, C.M. (2004). Contrast saturation in a neuronally-based model of elementary motion detection. *Neurocomputing*. (In Press)
Sinakevitch, I. & Strausfeld, N.J. (2004). Chemical neuroanatomy of the fly's movement detection pathway. *Journal of Comparative Neurology* **486**, 6–23.
Stavenga, D.G. (1979). Pseudopupils of compound eyes. In *Handbook of Sensory Physiology*, ed. Autrum, H., Vol. VII/6A, chapter 7, pp. 357–439. Berlin: Springer.
Sterling, P. (2002). How neurons compute direction. *Nature* **420**, 375–376.
Strausfeld, N.J. (1976). *Atlas of an insect brain*. Heidelberg, New York: Springer.
Strausfeld, N.J. & Campos-Ortega, J.A. (1977). Vision in insects: Pathways possibly underlying neural adaptation and lateral inhibition. *Science* **195**, 894–897.
Strausfeld, N.J. & Lee, J.K. (1991). Neuronal basis for parallel visual processing in the fly. *Visual Neuroscience* **7**, 13–33.
Torre, V. & Poggio, T. (1978). Synaptic mechanism possibly underlying directional selectivity to motion. *Proceedings of the Royal Society B* (London) **202**, 409–416.
Van Santen, J.P.H. & Sperling, G. (1985). Elaborated Reichardt detectors. *Journal of the Optical Society of America A* **2**, 300–320.
Wicklein, M. & Strausfeld, N.J. (2000). The organization and significance of neurons detecting change of depth in the hawk moth *Manduca sexta*. *Journal of Comparative Neurology* **424**(2), 356–376.

Appendix

In this appendix, we analyze the one-dimensional computational model shown in Fig. 3a in order to understand from where the spatial and temporal tuning properties arise, to make clear which computation each portion of the model performs, and to compare the response of the present model with the HR model shown in Fig. 3b, the analytical response of which is well known. This comparison will facilitate evaluation of the neuronally based EMD model against existing data based on the HR model.

Nondirectional motion: The Tm1 model

Consider the output of the model up to the level of Tm1 in response to a moving sinusoidal grating. If the center-to-center spacing of the photoreceptors is Δ, then the luminance inputs to the leftmost three photoreceptors shown in Fig. 3a from left to right may be expressed as

$$S_1 = 1/2\cdot[1 + C\sin(\omega_t t)],$$
$$S_2 = 1/2\cdot[1 + C\sin(\omega_t t + \omega_s \Delta)], \tag{A1}$$
$$S_3 = 1/2\cdot[1 + C\sin(\omega_t t + 2\omega_s \Delta)],$$

where C is the contrast, ω_t is the radian temporal frequency, t represents time in seconds, and ω_s is the radian spatial frequency. For brevity, we define the spatial phase factor $\phi_s = \omega_s \Delta$.

The first step in the model passes each photoreceptor signal through a high-pass filter. In this analysis, we neglect the small sustained response component in the amacrine-T1 pathway. Each pathway from the photoreceptors to the Tm1 unit also includes a single negative sign. We assume that the HPF completely removes the sustained component of the signal. The effect of the linear HPF on the remaining sinusoids is simply to multiply the amplitude by a frequency-dependent term $h_1(\omega_t)$ and to add a phase $\phi_1(\omega_t)$. Thus, the three signals after being high-pass filtered become

$$S_{H1} = -C/2\cdot h_1\cdot\sin(\omega_t t + \phi_1),$$
$$S_{H2} = -C/2\cdot h_1\cdot\sin(\omega_t t + \phi_1 + \phi_s), \tag{A2}$$
$$S_{H3} = -C/2\cdot h_1\cdot\sin(\omega_t t + \phi_1 + 2\phi_s).$$

The first and third signals are passed through a low-pass filter with magnitude response $h_2(\omega_t)$ and phase response $\phi_2(\omega_t)$, and thus the following three sinusoids arrive at the sum to produce the Tm1 model output.

$$S_{HL1} = -C/2 \cdot h_2 \cdot h_1 \cdot \sin(\omega_t t + \phi_1 + \phi_2),$$

$$S_{H2} = -C/2 \cdot h_1 \cdot \sin(\omega_t t + \phi_1 + \phi_s), \tag{A3}$$

$$S_{HL3} = -C/2 \cdot h_2 \cdot h_1 \cdot \sin(\omega_t t + \phi_1 + \phi_2 + 2\phi_s).$$

The sum of scaled and shifted sinusoids at the same frequency is always still a sinusoid. By use of common trigonometric identities, the amplitude of the sinusoid at the output of the Tm1 model may be shown to be

$$A_{Tm1} = C/2 \cdot h_1 \cdot \sqrt{4h_2^2[\cos^2(\phi_s) + \cos(\phi_s)] + 1}. \tag{A4}$$

The full model (Fig. 3a) makes use of two Tm1 cells, both of which have amplitude A_{Tm1}, and which can easily be shown to have a relative phase of ϕ_s. The expression for the absolute phase of each Tm1 output is complex and is not important to the final T5 output.

The above amplitude expression matches closely with a simulation of the one-dimensional Tm1 model, and explains the spatial and temporal frequency tuning of the Tm1 model shown in Fig. 8. The low temporal-frequency response of the model is dominated by h_1, the high-pass filter. At high temporal frequency the square-root term dominates the response and, while it follows a general trend to decrease at higher frequencies, the decrease is diminished relative to the low-pass filter response h_2. The spatial tuning around $\omega_s = 0$ results from the terms involving $\cos(\phi_s)$.

Directional motion: The T5 model

Because of the nonlinearity of the model from the Tm1 level to T5, we analyze its behavior separately from the rest of the model.

We know from the section above that the inputs to this model (for a moving sinusoidal grating input) are sinusoidal, have the same amplitude, and have a constant relative phase. We can express these two inputs as

$$I_1 = A_{Tm1} \cdot \sin(\omega_t t + \phi),$$

$$I_2 = A_{Tm1} \cdot \sin(\omega_t t + \phi + \phi_s), \tag{A5}$$

where the ϕ is the absolute phase of I_1 and $\phi_s = \omega_s \Delta$ is the relative phase of the two inputs.

Since the inhibitory interneuron used in the model results in a T5 model output that in the ideal case ($a = 0.5$) is one-half the difference between the inputs to the two T5 units [see eqn. (5) in Methods], we concentrate on computation of this difference. Passing the two inputs above through a low-pass filter with magnitude response $h_3(\omega_t)$ and phase response $\phi_3(\omega_t)$, we obtain

$$I_{1L} = h_3 \cdot A_{Tm1} \cdot \sin(\omega_t t + \phi + \phi_3),$$

$$I_{2L} = h_3 \cdot A_{Tm1} \cdot \sin(\omega_t t + \phi + \phi_3 + \phi_s). \tag{A6}$$

Making use of eqn. (3) for shunting inhibition (which normalizes the amplitude of the shunting input), the difference of the inputs to the two T5 units in Fig. 3a can be used to write the T5 model output as

$$\begin{aligned} 2 \cdot O_{T5} &= \mathrm{pos}[I_2] \cdot \left(1 - \frac{\mathrm{pos}[I_{1L}]}{I_{smax}}\right) - \mathrm{pos}[I_1] \cdot \left(1 - \frac{\mathrm{pos}[I_{2L}]}{I_{smax}}\right), \\ &= \mathrm{pos}[A_{Tm1} \cdot \sin(\omega_t t + \phi + \phi_s)] \\ &\quad \times (1 - \mathrm{pos}[A_{norm} \cdot \sin(\omega_t t + \phi + \phi_3)]) \\ &\quad - \mathrm{pos}[A_{Tm1} \cdot \sin(\omega_t t + \phi)] \\ &\quad \times (1 - \mathrm{pos}[A_{norm} \cdot \sin(\omega_t t + \phi + \phi_s + \phi_3)]), \end{aligned} \tag{A7}$$

where

$$A_{norm} = \frac{1}{I_{smax}} \cdot h_3 \cdot A_{Tm1} \tag{A8}$$

and I_{smax} is a constant equal to the maximum amplitude of the shunting inhibitory inputs

$$I_{smax} = \max_{\text{All } \omega_s, \omega_t} h_3 \cdot A_{Tm1}. \tag{A9}$$

We now concentrate on the temporal mean response of the model. Thus, multiplying out terms and removing two terms whose means cancel, we obtain

$$\begin{aligned} 2 \cdot \hat{O}_{T5} &= A_{Tm1} \cdot A_{norm} \cdot \mathrm{pos}[\sin(\omega_t t + \phi)] \cdot \mathrm{pos}[\sin(\omega_t t + \phi + \phi_s + \phi_3)] \\ &\quad - A_{Tm1} \cdot A_{norm} \cdot \mathrm{pos}[\sin(\omega_t t + \phi + \phi_s)] \\ &\quad \times \mathrm{pos}[\sin(\omega_t t + \phi + \phi_3)]. \end{aligned} \tag{A10}$$

By direct evaluation of the mean integral for each of the two terms below, it is possible to show that

$$\begin{aligned} \frac{8\pi \cdot \hat{O}_{T5}}{A_{Tm1} \cdot A_{norm}} &= [(\pi - \phi_{sum}) \cdot \cos(\phi_{sum}) + \sin(\phi_{sum})] \\ &\quad - [(\pi - \phi_{diff}) \cdot \cos(\phi_{diff}) + \sin(\phi_{diff})], \end{aligned} \tag{A11}$$

where

$$\phi_{sum} = |\phi_s + \phi_3|,$$

$$\phi_{diff} = |\phi_s - \phi_3|, \tag{A12}$$

and the principal value of each phase angle (that is, $0 < \phi_{sum}, \phi_{diff} \leq \pi$) is taken. Note that the absolute phase ϕ does not appear.

It is possible to approximate the term on the right side of eqn. (A11) as a product of sinusoids to get

$$\frac{8\pi \cdot \hat{O}_{T5}}{A_{Tm1} \cdot A_{norm}} \approx -\frac{5\pi}{4} \cdot \sin(\phi_s) \cdot \sin(\phi_3). \tag{A13}$$

While not exact, this expression is in error by less than 10% over the entire spatiotemporal frequency range of the model. Our simplified complete expression for the mean T5 output can now be written as

$$\begin{aligned} \hat{O}_{T5} &\approx -\frac{5 \cdot h_3}{32 \cdot I_{smax}} \cdot A_{Tm1}^2 \cdot \sin(\phi_s) \sin(\phi_3), \\ &= -\frac{5 \cdot C^2}{32 \cdot I_{smax}} \cdot [h_1^2 \cdot h_3 \cdot \sin(\phi_3)] \\ &\quad \times [(4h_2^2(\cos^2(\phi_s) + \cos(\phi_s)) + 1) \cdot \sin(\phi_s)], \end{aligned} \tag{A14}$$

where terms have been roughly grouped into temporal- and spatial-frequency response components.

Although approximate, the above expression is a very close match to the mean response of the one-dimensional neuronally based EMD model shown in Fig. 3a. The temporal-frequency response of the T5 mean output is the squared response of the Tm1 units multiplied by the magnitude and sine of phase of the low-pass filter used in the BL model. This narrows the temporal-frequency bandwidth, and gives a sharper cutoff at high temporal frequencies. The spatial-frequency response of the T5 mean, in addition to incorporating the square of Tm1 expression, has acquired a new term proportional to $\sin(\phi_s) = \sin(\omega_s \Delta)$. This term makes the T5 unit's spatial-frequency response null at zero spatial frequency (full-field flicker), unlike the Tm1 units.

Comparison with the HR model

Neglecting the rectifying step, it is possible to derive an analytical expression for the mean output of the HR model shown in Fig. 3b in response to the same sinusoidal stimuli used above. The rectification step does not greatly change the HR model general mean response properties, but obviously has a significant effect on the transient response to visual stimuli.

The expression for the mean response of the HR model to the stimuli of eqn. (A1) can be shown to be

$$\hat{O}_{HR} = -\frac{C^2}{36}\cdot[h_1^2\cdot h_4\cdot\sin(\phi_4)] \times [(4\cos^2(\phi_s/2) + 4\cos(\phi_s/2)\cos(3\phi_s/2) + 1)\cdot\sin(\phi_s)], \quad \text{(A15)}$$

where h_1 is the amplitude response of the HPF (the same filter used in the neuronally based EMD model), and h_4 and ϕ_4 are respectively the amplitude and phase response of the LPF used in the HR model. The terms of this expression have been grouped into temporal- and spatial-frequency response components.

While there is no direct equivalence between the temporal-frequency responses of the neuronally based EMD and HR models, the closest match between the two models is found when the HR LPF (h_4, ϕ_4) is second-order with poles matching those of the two low-pass filters used in the neuronally based EMD model. In this case, a good match in temporal frequency is obtained.

This same version of the HR model is the best match to the two-dimensional version of the neuronally based EMD model, in which each T1 unit integrates a hexagonal surround of amacrine inputs.